UNIVERSITY OF NAPLES FEDERICO II

DOCTORATE IN
MOLECULAR MEDICINE AND MEDICAL BIOTECHNOLOGY

XXXIII CYCLE

Carmen Caiazza

Knock-out of STING causes impairment of antigen presentation and abolishes STAT1 activation in mouse macrophages

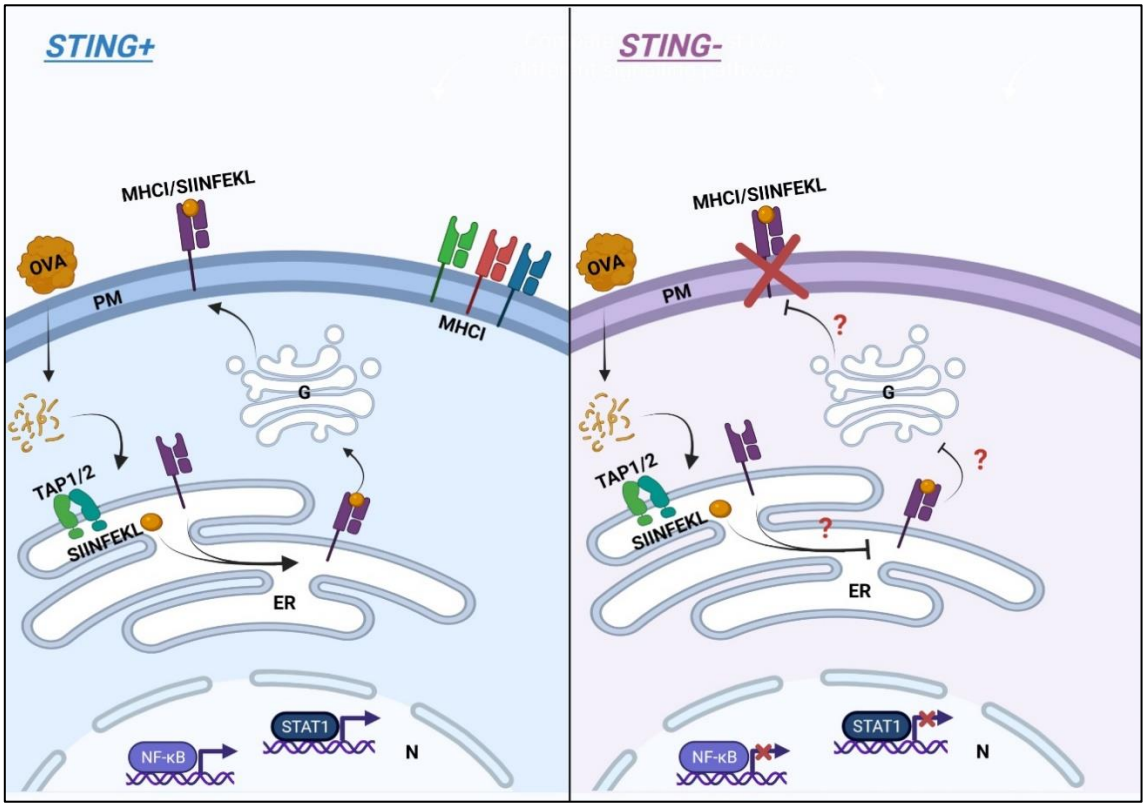

Year 2021

UNIVERSITY OF NAPLES FEDERICO II

DOCTORATE IN
MOLECULAR MEDICINE AND MEDICAL BIOTECHNOLOGY

XXXIII CYCLE

Knock-out of STING causes impairment of antigen presentation and abolishes STAT1 activation in mouse macrophages

Tutor
Prof. Massimo Mallardo

Candidate
Dott.ssa Carmen Caiazza

Year 2021

Table of contents

List of abbreviation

KO	Knock-Out
IFN	Interferon
LPS	Lipopolysaccharide
MHC	Major Histocompatibility Complex
Nf-κB	Nuclear Factor κ-light-chain-enhancer of activated B cells
OVA	Ovalbumin
PLC	Peptide loading complex
STAT1	Signal transducer and activator of transcription 1
STING	Stimulator of interferon genes
TAP1	Transporter associated with antigen processing 1
TAP2	Transporter associated with antigen processing 2
TAPBP	TAP binding protein
WT	Wild Type

Abstract

STimulator of INterferon Genes (STING) is a transmembrane ER resident protein involved in the interferon response to viral infection. Recent accumulating evidences show that the role of STING is not restricted to viral response but covers a broad range of processes. Here we assessed the role of STING in the MHC-I antigen presentation by generating mouse macrophages cell line, J774, STING KO. We observed an impaired OVA-derived SIINFEKL peptide presentation in STING KO cells. The defect is not caused by either uptake or processing of the ovalbumin. The analysis of the peptide loading complex showed an impaired gene expression of TAP1, TAP2 and TAPBP in STING KO though no differences in the protein expression were noticed. Co-IP assay upon OVA-treatment revealed no interaction between STING and TAP1. Cell surface levels of MHC-I were heavily decreased in STING KO macrophages. The mRNA expression of H2K1 heavy chain was not divergent between WT and KO whereas β2m light chain level was reduced in STING KO either at steady state and upon OVA treatment. Notably, STAT1 phosphorylation resulted impaired in KO upon OVA and LPS treatments. Moreover, the basal levels of STAT1 mRNA expression and protein were affected in the STING KO phenotype. Furthermore, OVA-induced STAT1 transcription was not observed in STING KO. We observed a reduction in CD11c cell surface levels in KO macrophages. In contrast, gene expression analysis revealed a basal higher level in STING KO and an OVA-induced increase. Finally, defects in Nf-κB activation and response to IFN-γ were observed in STING KO macrophages. Taken together these data confirm a role of STING in the antigen presentation that may occur either by regulating STAT1 signaling or by mediating the transport to the cell surface.

1. Background

During the evolutionary processes, vertebrates have developed different biological systems to fight infection of pathogens. The first line of defense is represented by the innate immunity. It comprehends a system of physical and chemical barriers, humoral and cellular effectors committed to fight the pathogen entrance and infection of the host. The host response to the infection begins with the sensing of pathogen which relies on a series of receptors distributed within the cell compartments known as pattern recognition receptors (PRRs). These receptors are able to recognize conserved structures among microbial species defined pathogen associated molecular patterns (PAMPs). PRRs include Toll-like receptors (TLRs), RIG-I-like receptors (RLR), nucleotide-binding domain and leucine-rich repeat-containing receptors (NLR), C-type lectin receptors (CLRs), cyclic GMP-AMP synthase (cGAS) and stimulator of interferon genes (STING). PRRs can be located on the cell surface as in the case of TLRs and CLRs or in the cytoplasm as RLRs, NLRs, CLRs and cGAS or as STING can be located in the intracellular membranes (Takeuchi 2010). Once activated by the sensing of pathogens, PRRs initiate the inflammatory response by activating proinflammatory cytokines, chemokines and interferons in order to counteract the infection (Takeuchi 2010).

TLRs were named after Drosophila melanogaster's Toll receptor discovered in 1990s as an essential receptor for defense against fungal infections (Lemaitre 1996). The human TLRs family consists of 10 receptors while in mice 2 more receptors have been identified. TLRs function as dimeric proteins in order to recognize a large number of microbial pathogens. TLR4, together with myeloid differentiation factor 2 (MD2), recognize lipopolysaccharide (LPS) a component of the outer membrane of Gram-negative bacteria. TLR2 forms heterodimers with either TLR1 or TRL6 to sense bacteria, mycoplasma, fungi and viruses. Besides, TLRs can sense RNA viruses both single-stranded (TLR7, TLR8) and double-stranded (TLR3). TLRs activation can result in two distinct pathways

depending on the adaptor molecule. The signaling via the adaptor MyD88 result in the activation of the transcriptional factors Nf-κB and AP-1 leading to the production of proinflammatory cytokines. The TRIF-dependent pathway act through the activation of two IKK-related kinases, TANK-binding kinase 1 (TBK1) and IKK-ε that phosphorylate the transcription factors IRF3 and IRF7 to induce interferons expressions (Takeuchi 2010).

The RIG-I-like receptor (RLR) family is composed by retinoic acid-inducible I (RIG-I), melanoma differentiation-associated gene 5 (MDA5) and laboratory of genetics and physiology 2 (LGP2) (Takeuchi 2009). This class of PRRs is localised in the cytoplasm and is involved in viral RNA sensing. All the members are characterized by a central helicase domain and an RNA binding domain. RIG-I and MDA5 also present a CARD domain which lacks in LGP2. The difference among the three protein relies on the length of the RNA recognized: while RIG-I senses relative short RNA (up to 1 kb), MDA5 detect longer dsRNA (more than 2 kb). LGP2 is involved in the regulation of the RLR signalling. It can act both as a positive regulator of its activation by unwinding RNA and facilitating RIG-I and MDA5 recognition, an as a negative one by sequestering RNA or inhibiting directly RIG-I. Upon activation the RLRs associate with the mitochondria antiviral signalling protein (MAVS) which via TBK1 and IKK-ε phosphorylation and consequent IRF3 and IRF7 nuclear translocation induce transcription of interferons (Rehwinkel 2020).

NLRs is a family of intracellular immune receptors that function by assembling in a large cytoplasmatic complex known as inflammasome. Pro-caspase-1 is recruited at the inflammasome and activated through autocatalysis. Through the cleavage of their immature form, caspase-1 activates IL-1β and IL-18 so causing endothelial cellular response and infiltration of immune cells to the damaged tissues. Moreover caspase-1 cleave gasdermin D to induce pyroptosis, a lytic proinflammatory cell death that act both exposing the

pathogens from their replicative niche and generating danger associated molecular patterns (DAMPs) so boosting the immune response. (Kelley 2019)

CLRs is a family of transmembrane receptor activated in response to viruses, bacteria and fungi. CLRs interact with pathogens by recognizing structures as mannose, fucose and glucan carbohydrate. Recognition by CLRs leads to the internalization of the pathogen, its degradation and subsequent antigen presentation. Once activated, CLRs cause activation of Nf-κB both directly and indirectly by interacting with TLRs (Geijtenbeek 2009).

Cyclic dinucleotide synthase is a cytoplasmatic DNA sensor that respond to the presence of DNA in the cytoplasm both of viral and host derivation. Upon activation it synthetizes 2'-3'-cGAMP which act as a second messenger to initiate the STING dependent production of interferons. (Li 2013)

1.1 The cGAS-STING pathway

cGAS belongs to the nucleotidyltransferase family, a class of enzymes which catalyze the transfer of a nucleotide monophosphate (NMP) from a nucleotide triphosphate (NTP) to an acceptor molecule. Specifically, cGAS converts GTP and AMP into the cyclic guanosine monophosphate–adenosine monophosphate (cGAMP), an unusual second messenger which contains phosphodiester linkages between the 2'-hydroxyl group of GMP and 5'-phosphate of AMP and the 3'-hydroxyl group of AMP and the 5'-phosphate of GMP (Kato 2013). DNA binding at the Zinc-ribbon domain of cGAS triggers a conformational change and dimerization that result in a rearrangement of its catalytic site (Zhang 2014). cGAS binding of DNA does not rely on the sequence but occur through the binding of the sugar phosphate backbone. Short DNAs are able to bind cGAS, but a longer sequence (>45 bp) is requested to form a more stable connection with cGAS dimers leading to stronger enzymatic activity (Luecke 2017). The

DNA binding induces the liquid phase condensation of cGAS and the formation of liquid droplets functioning as a microreactor in which the activated cGAS, and the substrates ATP and GTP are enriched. Once activated, cGAS catalyze the synthesis of 2',3'-cGAMP a ligand for the STING dimer (Du 2018).

STING is a protein of 42 kDa that localizes in the endoplasmic reticulum. It is composed by a short N-terminal cytosolic domain, 4 transmembrane domains, a cytosolic cyclic di-nucleotide (CDN) domain and a C-terminal tail (CTT) (Fig. 1). The CDN domain is the target of 2',3'-cGAMP which binds STING in dimeric form, adapting between 2 LBD. (Huang 2012)

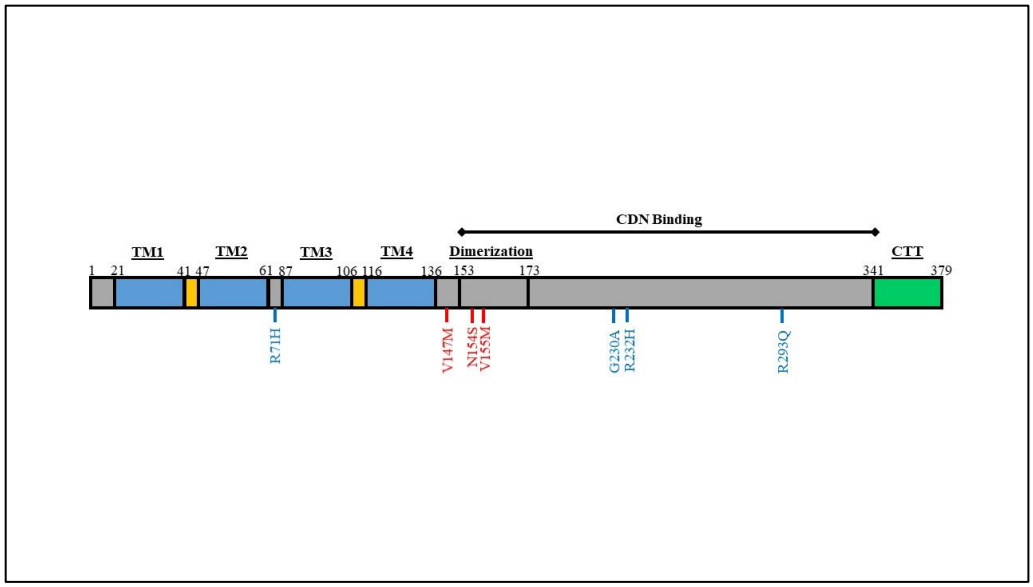

Fig.1 Schematic overview of STING,

STING is a 379 amino acids ER resident protein composed by a short N-terminal domain, 4 transmembrane (TM) domains, a cyclic dinucleotide (CDN) binding domain and a C-terminal tail (CTT). The common human STING variants (R71H, G230A, R232H and R293Q) are annotated in blue. SAVI associated mutation (V147M, N154S and V155M) are reported in red.

In resting state, STING is retained in ER through its interaction with the Ca^{2+} sensor stromal interaction molecule 1 (STIM) (Srikanth 2019). The binding of cGAMP disrupt this interaction and enhance that between STING and SEC24C, a component of the coat protein complex II (COPII) leading to its translocation from ER to Golgi apparatus via ER-Golgi intermediate compartment (ERGIC) (Fig. 2). (Dobbs 2015). Moreover, the binding of the ligand triggers a conformational change of STING with a 180° rotation of the CDN domain in relation to TM domain leading to the formation of STING oligomers composed by side-by-side packing of STING dimers. Furthermore, the CTT of STING is released and committed for the recruitment of the Tank-binding kinase 1 (TBK1) on its TBK1-binding motif (TBM). (Shang 2019) Multiple TBK1 dimers are recruited by the STING oligomer and activated by trans-autophosphorylation. Because of the difference in size between TBK1 and STING it has been proposed that TBK1 is recruited sub-stoichiometrically leaving fraction of the oligomer unbound with TBK1. Upon activation, TBK1 phosphorylates serin 366 in the pLxIS motif of the unbound human STING CTT (Ser365 of mouse STING). The phosphorylation of this motif function as a docking site for IRF3 recruitment, via interaction with its positively charged surface, and phosphorylation by TBK1. At this point, IRF3 dimerizes and enter the nucleus to initiate type I Interferon (IFN-I) response leading to the expression of a set of interferon stimulated genes (ISGs) and the establishment of antimicrobial immunity (Liu 2015) (Fig. 2).

In addition to IRF3, the activation of cGAS-STING signaling also leads to Nf-κB activation (Fig. 2). The regulation of Nf-κB relies upon TNF receptor-associated factor 6 (TRAF6), Nf-Kb essential modulator (NEMO), IKKβ and TBK1 (Abe 2014; Fang 2017).

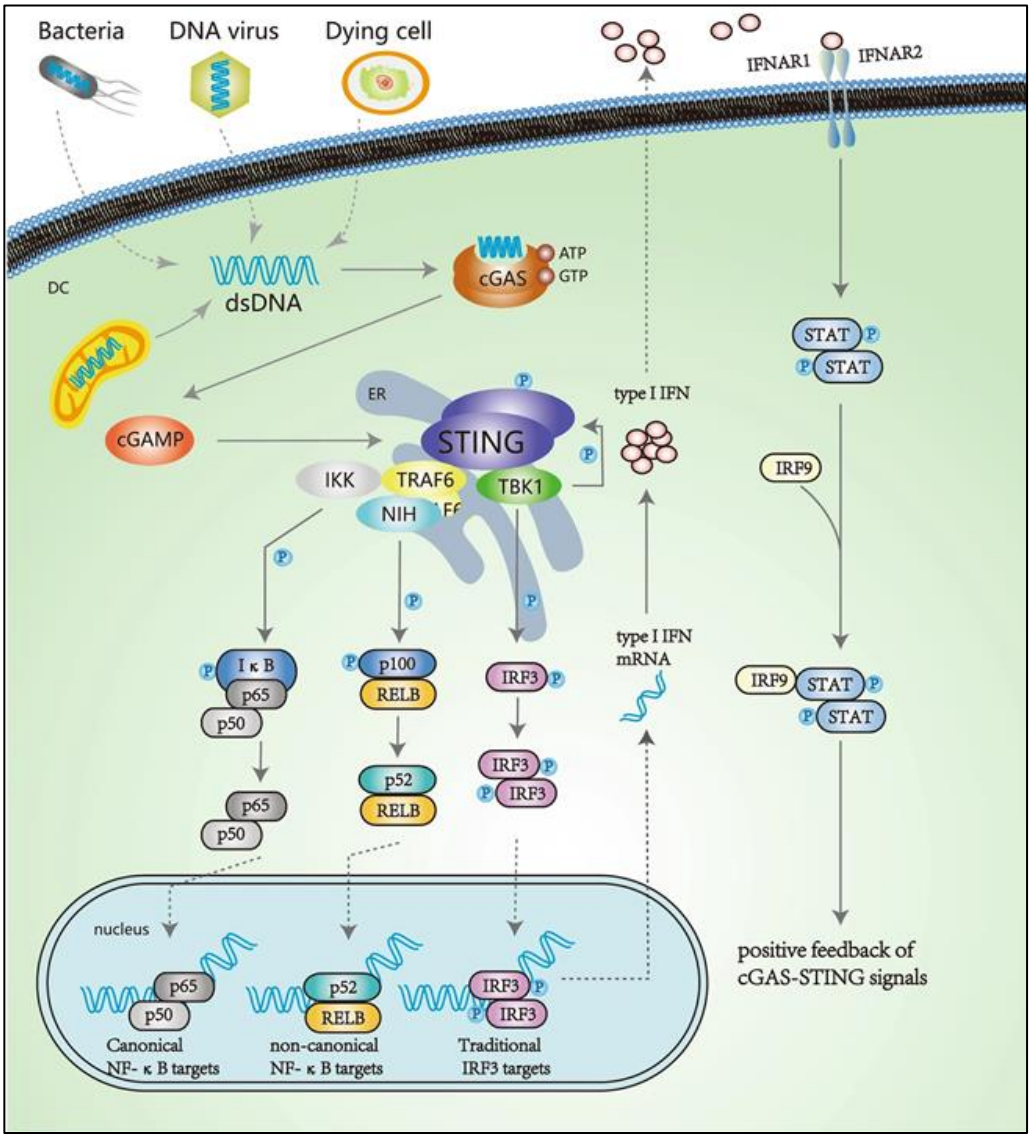

Fig.2 The cGAS-STING pathway.

dsDNA derived by mitochondria, dying cells or pathogens is detected by cGAS which synthetize cGAMP to activate STING. Upon activation, STING translocate from ER to Golgi apparatus where it recruits TBK1, IKK and TRAF6 leading to the phosphorylation and nuclear translocation of IRF3, p52/RelB and p65/p50. In the nucleus IRF3 activates the production of IFNs-I which via binding to IFNAR1 and IFNAR2 activate STATs inducing the transcription of ISG. (Wang et al., 2020)

The cGAS-STING pathway may also trigger the phosphorylation and activation of signal transducer and activator of transcription 6 (STAT6). Upon interaction with STING and phosphorylation by TBK1, STAT6 dimerize and translocate to nucleus to induce the expression of a series of chemokines as CCL2, CCL20 and CCL26 which are important in eliciting antiviral responses (Chen 2011).

Besides the canonical signaling triggered by cGAMP, it has been reported that STING can be activated by other DNA sensors as IFNγ-inducible protein 16 (IFI16), DEAD-box helicase 41 (DDX41), DNA-dependent protein kinase (DNA-PK) and heterogeneous nuclear ribonucleoprotein A2B1 (hnRNPA2B1). These mechanisms may represent a strategy to counteract the pathogen's evasion from DNA sensors but are still poorly understood. (Zhang 2011; Unterholzner 2010; Ferguson 2012; Wang 2019)

Apart from cGAMP other CDNs, including c-di-AMP, c-di-GMP and 3',3'-cGAMP, directly produced from the bacteria can trigger the activation of STING bypassing DNA sensors however the effects of these uncanonical activation are different depending on the cellular context (Whiteley 2019).

It has been reported that STING participates to RNA viruses response by interacting with RIG-I and MAVS. Nazmi et al (2012) demonstrated that deletion of STING impairs RIG-I mediated innate signaling.

Moreover, despite the mechanism is still unknown, it has been reported that virus-cell fusion can activate STING in a DNA independent way (Holm 2012).

The triggering of STING may occur also indirectly. For example, the mitochondrial stress with consequent release of mitochondrial DNA (mtDNA) induced by infection of Herpes simplex 1 (HSV-1) corroborate STING activation during the infection (West 2015).

1.2 Evolution of cGAS-STING pathway

Despite the role of STING is mostly studied in mammals, specifically in human and mouse, the primary sequence of both cGAS and STING have been identified in *Monosiga brevicollis*, a choanoflagellate belonging to the Codonosigaceae family considered the closest unicellular relatives of animals (Wu 2014).

A c-GAS-like enzyme dinucleotide cyclase (DncV) has been found in Vibrio cholerae. Upon phage infection DncV catalyzes the production of 3',3'-cGAMP which act as agonist for the c-GAMP-activated phospholipase (CapV) leading to membrane degradation and cell death so preventing the propagation of the phage (Severin 2018).

Bioinformatic analysis have displayed a wide distribution of cGAS and STING homologues across animal species though differences have been found (Wu 2014). Invertebrates cGAS lacks the zinc-ribbon domain resulting in its inability to bind DNA. Moreover, the CTT of STING fundamental to trigger the IFN signaling is also absent in invertebrates (Qiu 2018). Taken together these data seem to suggest a different ancient role of STING significantly different from the canonical described in vertebrates but still related with antiviral immunity. In Drosophila melanogaster the production of CDNs during the infection by *Listeria monocytogenes* trigger the dmSTING activation. Once activated dmSTING induces the production of antimicrobial peptides through the Nf-κB factor Relish (Martin 2018). It has been demonstrated a role of dmSTING even in protecting the host from RNA infection through autophagy and Nf-κB activation (Liu 2018, Goto 2018). Even though the mechanism is still unknown mutation of residues R232 and F234, corresponding to CDN binding site in hSTING, impaired the antiviral activity suggesting that CDNs may function directly activating STING (Goto 2018).

In vertebrates despite the structural domains of cGAS and STING are conserved among the species the proteins display significant differences. Human

cGAS (h-cGAS) display a high preference for binding longer DNA compared to mouse cGAS (m-cGAS). This specificity is imputed to the presence of two specific residues in h-cGAS K187/L195. Indeed, by deleting these residues h-cGAS lose the ability of preferentially binding long DNA whereas inserting these residues in m-cGAS confer the same long DNA recognition restriction. Interestingly the deletion in h-cGAS result in impaired enzyme activity which could be a compensation to avoid overactivation that could lead to excessive immune response (Zhou 2018).

As reported for cGAS, m-STING and h-STING display significant differences particularly in ligand selectivity. h-STING display greater preference for 2',3'-cGAMP then for 3',3'-cGAMP or c-di-GMP compared to mSTING (Ablasser 2013). Moreover, while the designed drug for antiviral therapies DMXAA fails to target h-STING, it works well for m-STING (Shih 2018).

The STING human protein, encoded by TMEM173 gene at 5q31.2, display a very heterogeneity in its alleles. The most common variant is characterized by the presence of an arginine at amino acid 232 (R232). Other common alleles are HAQ (R71H-G230A-R293Q), AQ (G230A-R293Q), Q293 and H232. The alleles have a significant population stratification. Most of Europeans have R232/R232 genotype while in East Asia the most common is HAQ/R232. The HAQ/HAQ is present in about 16% of Asians and about 3% of Europeans while lacks in Africans which instead display the AQ/AQ genotype in 4% of the population. (Jin 2011) H232 is defective in response to CDNs while individuals with HAQ display a decreased TMEM173 transcripts (Burdette 2011, Patel 2017).

1.3 Noncanonical roles of STING

Following the evidence of STING ancient function beyond DNA sensing its role in autophagy has been further investigated. It has been reported that STING-induced autophagy is important for the clearance of cytosolic DNA in order to avoid an induction of autoimmunity (Fig. 3A and D). The STING-containing ERGIC is a membrane source for LC3 lipidation mediated by WD repeat domain phosphoinositide-interacting protein (WIPI2) and autophagy protein 5 (ATG5) (Gui 2019). Moreover, in Drosophila melanogaster STING dependent autophagy is important for protection from Mycobacterium tuberculosis, Gram positive bacteria and Zika virus infection (Moretti 2017, Watson 2015, Liu 2018).

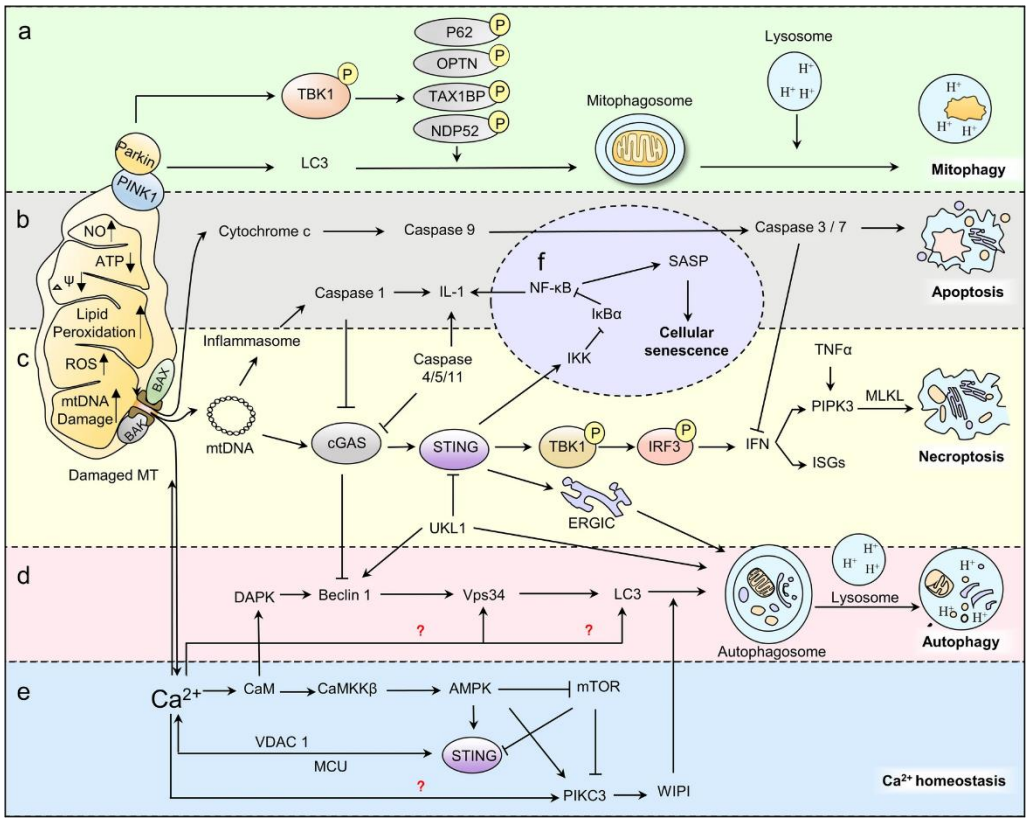

Fig.3 cGAS-STING pathway participates to the regulation of physiological processes. (Gao 2020)

Beyond the noncanonical role in autophagy it has been demonstrated that STING participates in the unfolded protein response (UPR). ER induced stress during alcoholic liver disease resulted in induction of IRF3 dependent apoptosis triggered by STING (Patrasek 2013). The induction of STING during infection from *Mycobacterium bovis* and *Brucella abortus* is dependent on UPR (Cui 2016, Guimares 2019). Besides Guimares et al (2019) demonstrated that the STING and UPR regulates themselves with a reciprocal crosstalk: UPR activates STING and viceversa. The induction of STING during infection from *Mycobacterium bovis* and *Brucella abortus* is dependent on UPR (Cui 2016, Guimares 2019). Besides, during Brucella infection the UPR was lower in STING -/- cells (Guimares 2019). Furthermore, ER stress induced by angiotensin II is dependent on STING and KO mice have a reduced ER stress after aorting banding (Zhang 2020).

Finally, the cGAS-STING pathway has also been correlated with mechanism of cell death induction (Fig. 3B). Gaidt et al (2017) reported that STING is able to trigger NOD-, LRR- and NLRP3 depending cell death. Even apoptosis in T cells, malignant B cells and naïve B cells could be induced by STING upon activation (Cerboni 2017, Tang 2016). Brault et al (2018) demonstrated that in bone marrow derived macrophages STING is able to trigger the RIPK3 dependent necroptosis (Fig. 3C).

1.4 Post-translational control of the cGAS-STING pathway

The delicate balance between the elimination of pathogens and the prevention of overactivation that could harm the host is maintained by post-translational modification (PTMs) of the effectors involved in immune response. In the cGAS-STING pathway the PTMs modification can occur at any step of the signaling. Besides, the covalent modification can function both positively by

enhancing the activation and negatively by terminating the signal. The PTMs of the cGAS-STING signaling are summarized in Table 1.

In resting cells cGAS is maintained inactive by several PTMs as glutamylation, acetylation, sumoylation and ubiquitination. Tubulin tyrosine ligase-like 4 (TTLL4) dependent monoglutamylation impairs the synthase activity of cGAS while TTLL6 act on DNA binding affinity (Xia 2016). Acetylation of cGas at K384, K394 and K414 is the mechanism by which aspirin suppress self-DNA-induced autoimmunity in Aicardi-Goutières syndrome (AGS) (Dai 2019). Together with K414 acetylation, sumoylation of K217 antagonize K48-linked ubiquitination (Hu 2016). Either STING is maintained inactive by the ubiquitin-specific protease 13 (USP13) by deconjugation of K27-linked polyubiquitin chains (Sun 2017).

In response to stimuli, histone deacetylase 3 (HDAC3), cytosolic carboxypeptidase 5 (CCP5) and CCP6 remove the inhibitory acetylation, monoglutamylation and polyglutamylation respectively (Xia 2016, Dai 2019). These residues previously occupied by inhibitory modification undergo to monoubiquitination by tripartite motif-containing 56 (TRIM56) and K27 ubiquitination by ring finger protein 185 (RNF185) resulting in enhancing cGAS activity (Seo 2018, Wang 2017).

The relased CTT of STING is modified by several PTMs. Sumoylation by TRIM38 facilitates STING oligomerization and mask an adjacent motif recognized by heat-shock cognate protein 70kDa (HSC70) which mediates its degradation via chaperon mediated autophagy (Hu 2016).

Several ubiquitination may occur on STING. According to the type of ubiquitination at K150, K48-linked or K11-linked by RNF 26, the STING protein levels after viral infection are maintained balanced (Qin 2014). K27 and K63-linked polyubiquitination potentiate TBK1 recruitment and its downstream signal. In particular K63-linked polyubiquitination at K224 by mitochondrial E3

ubiquitin ligase (MUL1) is specifically required for STING trafficking and a prerequisite for its phosphorylation and degradation (Ni 2017).

Protein	*Modification*	*Residues*	*Enzyme*	*Functions*
CGAS	Monoubiquitination	K335	TRIM56	Dimerization
	K27 polyubiquitination	K173 K384	RNF185	↑ Enzimatic activity
	Phosphorylation	S305	AKT	↓ Enzimatic activity
	Polyglutamylation	E272	TTLL6	↓ DNA binding
	Deglutamylation	E272	CCP6	Reverse inhibition
	Monoglutamylation	E302	TTL4	↓ Enzimatic activity
	Deglutamylation	E302	CCP5	Reverse inhibition
	Deacetylation	K384	HDAC3	Reverse inhibition
	Desumoylation	K479	SENP2	↑ Degradation
STING	K11 polyubiquitination	K150	RNF26	Stabilization
	Deubiquitination	N.D.	USP13	Block TBK1 recruitment
	K63 polyubiquitination	K224 K236 K289 K338	MUL1	Dimerization
	Deubiquitination	N.D.	USP21	Inhibits the STING-TBK1-IRF3 complex
	K48-polyubiquitination	K275	TRIM30α	Degradation
	K48-polyubiquitination	K150	RNF5	Degradation
	Phosphorylation	Y245	SRC	↑ Activation
	Phosphorylation	S358	TBK1	Facilitate aggregation
	Phosphorylation	S366	TBK1	Recruitment IRF3
	Phosphorylation	S366	ULK1	Degradation
	Dephosphorylation	Y245	PTPN1/2	Degradation
	Palmitoylation	S358	PPM1A	Impairs aggregation
	Sumoylation	C88/91	DHHC	↑ IFN-I response
	Desumoylation	K338	TRIM38	Oligomerization
	Desumoylation	K338	SENP2	Degradation

Table 1. Post transcriptional modifications of cGAS-STING.

Upon activation STING phosphorylation at S366 (S365 in mouse) is critical to induce IRF3 mediated response (Liu 2015). Two additional phosphorylation sites at Y245 and S358 has been found to fuel STING activation (Li 2015).

In addition, STING palmitoylation at Cys88 and Cys91 in TGN is required for STING oligomerization and IFN responses (Mukai 2016). Three prime repair exonuclease 1 (Trex1)-deficient mice treated with small molecules which covalently modify these residues display an improvement of autoinflammatory phenotypes due to an overactivation of STING caused by spontaneous dimerization (Haag 2018).

In order to disrupt the flawless mechanism armed against the invasion and spread the infection, pathogens have developed several strategies to evade from the host immune response. The main mechanisms by which microorganism act this evasion are accomplished via the avoidance of DNA exposure by recruiting host factors or directly by inhibiting the signaling at any step.

1.5 Pathogen evasion from the cGAS-STING pathway

Once entered the cell, HIV-1 initiate the reverse transcription of its genomic RNA into dsDNA which is then transported to the nucleus. HIV-I recruits host factors as CPSF6 and cyclophilins to attenuate viral DNA synthesis in the cytosol avoiding the detection by cGAS and so facilitating the nuclear entry (Rasaiyaah 2013).

The target of cGAS for its inhibition can occur in several ways. HSV-1 use more than one of its proteins to avoid the cGAS detection, each one with a different assignment. UL41 act by inducing degration of cGAS mRNA impairing the levels of the available protein. VP22 dampens its enzymatic

activity with an unknown mechanism and UL37 compromise its activity through PTMs modifications (Su 2017, Huang 2018, Zhang 2018).

Vaccinia virus (VACV) F17 protein cause cGAS degradation in mTOR dependent way (Meade 2018).

The chosen target of pathogens to avoid the sensing can be also the second messenger cGAMP. Some microorganisms as Mycobacterium and Streptococcus use CdnP phosphodiesterase to enzymatic cleave CDNs (Dey 2017). Similarly, through the nuclease poxin VACV hydrolyze 2'3'-cGAMP (Eaglesham2019).

The downregulation of STING can occur with different strategies. Some flaviviruses, as DENV, proteolytically cleave STING through the protease complex NS2B3 (Kim 2017). Other viruses, as Hepatitis C virus and coronavirus HCoV-NL63 interfere with its oligomerization (Yi 2016, Sun 2012). Another approach used by pathogens consist in interfering with its ubiquitination as executed by human T-lymphotrophic virus 1 and Yersinia (Wang 2017, Cao 2016). Several viral proteins, as UL82 and UL42 of HCMV, target the iRhom2/TRAPβ complex which is responsible of STING trafficking from ER to Golgi (Luo 2016). The first act by disrupting the complex while the latter by inducing TRAPβ degradation (Fu 2017, Fu 2019).

HSV-I regulation of STING seems to be contradictory. While UL46 negative regulate STING protein levels, other proteins as ICP0, ICP4 and US3-PK have been reported to stabilize STING (Kalamvoki 2014, Deschamps 2017). Taken together these data suggest that the role of STING in HSV-1 infection is dependent on the cell type.

The negative regulation can occur also on STING downstream targets. KSHV block the interaction between STING and TBK1 (Ma 2015). ICP27 of HSV-1 associates with STING/TBK1 complex and prevent IRF3 phosphorylation and IFN signaling (Christensen 2016).

Beside the direct modulation of STING, HSV-1 can also inhibit Nf-κB activation with two different approaches. UL36USP stabilizes IκBα repressor while UL24 inhibits its nuclear translocation (Ye 2017, Xu 2017).

Intriguingly, some pathogens rather than mediate STING inactivation cause its activation. *Listeria monocytogenes* after the invasion release c-di-AMP into the cytosol of the infected cell leading to STING activation. This indicates that in some way pathogens can modulate STING activity for their own benefits (Archer 2014).

1.6 STING in regulation of calcium homeostasis

Recent evidences have connected the dysregulation of Ca^{2+} signaling with the insurgence of autoimmune disease. DNA-dependent activator of interferon genes (DAI) interacts with self-DNA derived from apoptotic bodies, genome instability and mitochondrial damage triggering the cGAS-STING response. The inhibition of Ca^{2+} signaling acting on both the release from the ER and mitochondrial export during DAI-mediated signaling dampened the immune response (Zhang 2013). Reduction of cytoplasmatic Ca^{2+} result in reduced IRF3 and NF-κB activation suggesting that the DAI-cGAS-STING signaling is important in the insurgence of autoimmune diseases. It was hypothesized that the activation of IRF3 and NF-κB downstream STING are regulated by calmodulin (Fig. 3E). This was supported from data displaying that treating macrophages with W-7 a potent calmodulin inhibitor result in a reduction of IFNs production (Gamage 2017). These data, together with other evidences of impaired Ca^{2+} modulate signaling in other autoimmune diseases has prompt the researchers to deep analyze the connection of calcium mediated signaling with proteins involved in immune response.

It has been showed that STING monomers share a two Ca^{2+} binding sites during dimerization and that the calcium binding is fundamental for triggering the activation. Specifically, the binding occurs between Glu316 and Asp320 side chain of one monomer and Asp205 and Ala318 of the other. When the corresponding amino acids (Glu315 and Asp204) lack in mice, STING is unable to trigger its downstream signaling (Shu 2012). However, the precise mechanism of STING and calcium interconnection is still not well understood and quite controversial. The release of a precise amount of calcium into the cytoplasm seems to be a master regulator of this delicate balance. A too low level of calcium is not sufficient for triggering STING activation, but saturating levels seems to inhibit STING activation (Kwon 2018).

To strengthen this hypothesis, it has been demonstrated that in resting state STING physically interacts with STIM1 an ER transmembrane protein involved in the release of calcium. STIM1 retain STING into ER so preventing its activation. Upon stimulus STIM translocate to plasma membrane and interact with ORAI1 channels causing extracellular calcium afflux into the cell. Beside, STIM1 translocation release STING from the anchorage to the ER. The inhibition between STING and STIM is mutual: STIM keep STING anchored to ER membrane while STING inhibit STIM translocation at plasma membrane. In some cell types as MEFs and Jurkat the loss of STING causes an enrichment of STIM at plasma membrane with consequent dysregulated afflux of Ca^{2+} (Srikanth 2019).

Lee el al (2013) reported that STING also interact with ATP2A2 a SERCA Ca^{2+}-ATPase localized on ER responsible for sequestration of calcium from the cytosol associated with the muscular contraction (Lee 2013).

Moreover, a study conducted by Sixt et al (2017) further elucidate the role of STING as a mediator in Ca^{2+} regulation. During infection *Chlamydia trachomatis* induce host cell death through increasing of intracellular Ca^{2+} with a STING-dependent mechanism without induction of IFNs. SERCA inhibition

using pharmacological inhibitors prevent the STING-dependent cell death (Sixt 2017).

Apart from the direct activation, STING can be activated by calcium indirectly in a process that involve the calmodulin signaling. Calcium binds and activates Calcium/calmodulin dependent protein kinase II (CAMKII) which phosphorylates AMPK. AMPK inhibits ULK1 through phosphorylation hampering the negative regulation of STING (Konno 2013). Because of the activation of STING leads to a release of calcium in the cytosol due to the release of STIM, once triggered, STING begin a positive loop by activating CAMKII.

Moreover, the increase of cytosolic Ca^{2+} triggers the mitochondrial-permeability transition (MPT) leading to the leakage of mtDNA into the cytoplasm inducing the cGAS-STING signaling. In 2013 Zhang et al demonstrated the connection between MPT and STING induction. The use of cyclosporin A, an inhibitor of MPT, suppresses the STING-mediated activation of IFNs in macrophages (Zhang 2013). However, there is still debate about this because reports show that agonist-mediated STING activation require an intact mitochondrial membrane potential for a correct induction of IFNs response (Prantner 2012).

Shoshan-Barmatz et al (2017) enlightened a possible role of STING in mediating calcium release by mitochondria. Because of its direct interaction with voltage-dependent anion selective channel 1 and 3 (VDAC1 and VDAC3), two ion channels resident in the outer mitochondria membrane involved in Ca^{2+} uptake by mitochondria, it has been suggested that in a similar way to ATP2A2 STING could modulate the Ca2+ release from the mitochondria (Shoshan-Barmatz 2017).

1.7 STING in autoimmune inflammatory diseases

Because of its junctional role in the response to infection a precise regulation of STING appears to be fundamental to maintain the delicate equilibrium between active and inactive state of the immune response. Dysregulation of the immune response due to STING overactivation can lead to a continuous stimulation of inflammatory proteins which can result in the development of autoimmune and autoinflammatory disorders. It has been amply demonstrated that an overactivation of the cGAS-STING signaling results in the development of different autoimmune disorders. The dysregulation can result either by direct mutation in effector proteins of the signaling or by an impairment of its regulators. The first mechanism involved in the regulation of the signaling is relies on the maintenance of the nucleic acid clearance into the cell. For this purpose, a series of nucleases that keep the level of self-DNA under the threshold of activation, are triggered: the activation of cGAS occurs only when the concentration of cytosolic DNA overcome that threshold. The derivation of it can be either exogenous and endogenous. In addition to the release of the genome into the cytoplasm, most of viral infection cause a mitochondrial stress leading to the release of mtDNA that intensify the activation of cytosolic PRRs.

TREX1 is responsible of the hydrolyzation of cytosolic DNA. Mutations in this gene has been associated with a series of autoimmune disorders as Aicardi-Goutieres syndrome (AGS), systemic lupus erythematous (SLE), familial chilblain lupus and retinal vasculopathy with cerebral leukodystrophy (Crow 2006, Rice 2005). All these syndromes are characterized by high levels of ISGs suggesting that the clinical manifestation relies upon the overactivation of IFNs signaling. As expected, the seriousness of clinical manifestation in TREX1 -/- mouse model is attenuated either by KO of cGAS or by crossing the mouse with a STING -/- (Gao 2015, Morita 2004).

DNAseII is a lysosomal endonuclease responsible for the elimination of DNA derived from dead cells, developing red blood cells and expelled nuclei engulfed

by macrophages (Kawane 2001). DNaseII KO mice die before birth because of the excessive production of IFNs triggered by nuclear DNA expelled from erythroid progenitors. The embryonic lethality can be rescued by knocking out IFNARI, cGAS and STING (Kawane 2006, Gao 2015, Ahn 2012).

Gain of function mutations of STING cause the STING-associated vasculopathy with onset in infancy (SAVI). This syndrome is characterized by systemic inflammation, peripheral vasculitis, skin inflammation and pulmonary manifestation. The clinical manifestations are triggered by the elevated expression of IFN-β and excessive levels of interferon-induced cytokines (Liu 2014). The three most common SAVI-associated mutation of STING are V155M, N154S and V147L. These mutations are localized in the connector helix between the TM and LBD. The substitution of these amino acids causes a spontaneous rotation of LBD motif resulting in STING constitutive activation (Liu 2014). More recently other mutation has been found in the tetramer oligomerization region mapping on Cys206, Arg281 and Arg284 (Melki 2017). The mouse model of the disease display T cell cytopenia and disfunction. Unexpectedly the pathological phenotype is not rescued neither by IFNARI or IRF3 deletion (Bouis 2019, Warner 2017).

1.8 STING in chronic SNC pathologies

The deepest knowledge of the cGAS-STING signaling together with the discovery of its non-canonical activation has aroused the interest around the possible involvement in a series of pathologies somehow related to inflammation. Recent accumulating studies report STING signaling involvement in several chronic neurodegenerative diseases. Nazmi et al (2019) demonstrated that in mice models of neurodegenerative diseases, the neuroinflammation downstream IFN-I overactivation is attenuated when

deleting STING or IFNAR1. Parkinson disease's mouse model is characterized by the lacking of ubiquitin ligase PARKIN. The lack of PARKIN result in an increasing of circulating mtDNA due to an inefficient clearing of damaged mitochondria (Sliter 2018). Sliter et al (2018) demonstrated that by deleting STING, mice display an improvement of phenotype with reduction of neuroinflammation and neurodegeneration. Similarly, an increase of free circulating mtDNA has been described in mouse models of ataxia-telangiectasia (ATM) (Hartlova 2015).

Besides, cGAS-STING signaling has been connected with Huntington disease (HD). In striatal neurons of Huntington disease's patients increased levels of cGAS protein has been found. Sharma et al (2020) established an increasing of of p-STING and p-TBK1 in the striatal neuron derived from HD mice model. Moreover, the increasing of Ccl5 and Cxcl10 mRNA levels has been found to be dependent upon cGAS-STING pathway further corroborating its role in the induction of the neuroinflammation (Sharma 2020).

Similarly, spinal cords of amyotrophic lateral sclerosis (ALS) patients display elevated levels of cGAMP. Recently Yu et al (2020) have demonstrated a physical interaction between STING and TDP-43 a hallmark protein of ALS. Moreover, cortex of TDP-43 overexpressing mice has been found enriched with both cGAS and cGAMP (Yu 2020).

In accordance with the controversial role associated to STING, in some chronic neurodegenerative diseases it seems to exert a neuroprotective role. In mouse model of multiple sclerosis, the activation of STING both by CDNs and the antiviral ganciclovir induces neuroprotection and reduce of inflammation (Lemos 2014, Mathur 2017).

Finally, the cGAS-STING pathway has been related with age induced inflammation. Hutchinson-Gilford progeria syndrome (HGPS) is a premature ageing disease caused by the production of progerin, a truncated form of lamin A. Lan et al (2019) have described an increase of cytosolic DNA in HGPS

patients compared to healthy donor suggesting that the trigger of the signals downstream cGAS-STING could be related with the pathology.

1.9 STING in Cancer

Following the recent accumulating evidences that connect the cGAS-STING pathway with an increasing number of physiological and pathological mechanism it is not unexpected that it has been found related with the pathogenesis of cancer.

Genomic instability, a hallmark of cancer cells, induce the formation of micronuclei a membrane-enclosed perinuclear package of damaged DNA formed during mitosis. The rupture of such agglomerates leads to activation of cGAS (Mackenzie 2017). Kitai et al (2017) suggested that the leakage of DNA from micronuclei is the first step of a mechanism used to transport via exosomes tumor DNA to the nearby dendritic cells in order to produce an antitumor response (Kitai 2017). Moreover, it has been demonstrated that immune cells could receive tumor derived cGAMP through gap junction or SLC19A1 (Luteijn 2019, Chen 2016). Despite this, the role of the axis cGAS-STING in cancer is still controversial: it seems to be able to lead both to an antitumor response and to the tumoral progression by inducing the development of metastasis. The different effects seem to rely upon the timing of the activation. In early stages the presence of cytosolic DNA triggers the immunosurveillance and induce cancer senescence. However, once the tumor acquires the ability to evading immune response activation of cGAS-STING axis result in chronic inflammatory associated with pro-survival and metastasis. Beside the timing, other mechanisms are able to modulate its downstream effects during the tumoral progression. Chon et al (2019) demonstrated that low expression of cGAS in colorectal cancer is a hallmark of a more advanced stage of the tumor. Similarly,

in advanced gastric cancer both mRNA and protein levels of STING are reduced (Song 2017). On the contrary both cGAS and STING result upregulated in breast, prostate and head-and-neck tumors (Liang 2015, Gaston 2016, Haughey 2020).

The antitumoral effect of cGAS-STING can be accomplished through different mechanism. It can boost the response of adaptive immune cells by activating natural killer (NK) cell response and priming T lymphocytes for tumor surveillance (Marcus 2018, Woo 2014). Corrales et al (2015) showed that in dendritic cells, the activation of STING upon tumor DNA recognition leads to type I IFNs production enhancing tumor antigen presentation so leading to the priming of CD8+ T cells (Corrales 2015). Furthermore, its activation by chemotherapy and radiotherapy can induce senescence-associated secretory phenotype (SASP) so restricting tumorigenesis (Gluck 2017).

The counterpart is that tumor cells with high chromosomal instability use the overactivation of the cGAS-STING axis to induce tumor invasion and metastasis. The metastatic phenotype is induced by the activation of noncanonical Nf-κB signaling (Bakhoum 2018). Moreover, according to Chen et al (2016), cGAMP is transferred via gap junction from brain tumor to astrocytes. This translocation induces the secretion of IFNα and TNFα with the consequent activation of STAT1 and Nf-κB promoting metastasis and chemoresistance (Chen 2016). Furthermore, Liu et al (2018) demonstrated that the cGAS dependent suppression of homologous repair (HR) promote tumorigenesis. Upon DNA damage, cGAS undergo to nuclear translocation and is recruited to the site of double strand break inducing non homologous end joining (NHEJ) which promote the development of new potentially tumorigenic mutations (Liu 2018).

Finally, the promotion of tumor immune evasion has also been connected with an overactivation of cGAS-STING signaling. In particular the stimulation

induces the recruitment of T-reg and immunosuppressive proteins as PDL1, CCR2 so preventing the antitumoral immune response (Fu 2015, Liang 2015).

1.10 Targeting the cGAS-STING pathway for therapeutic approaches

The established roles of cGAS-STING signaling in the development of several diseases has aroused a great interest on its pharmacological regulation in order to counteract the pathological manifestation. Potentially the regulation of the cGAS-STING axis, both in positive and in negative depending on its dysregulation, could be a beneficial approach for a wide spectrum of diseases as cancer, neurodegeneration, chronic viral infection, autoinflammatory and autoimmune diseases.

In cancer, depending on the pro- or anti- tumoral role of the signaling several approach using both agonists and antagonists have been developed. It has been established that, beside the cytostatic effect, the beneficial action of most of chemotherapeutic and radiotherapeutic approaches rely on the release of cytoplasmic DNA with the consequent induction of the cGAS-STING dependent induction of antitumoral immune response.

The antitumoral effects of STING agonists are explicated either by improving the immunosurveillance via the stimulation of the T cell proliferation and by the induction of apoptosis in tumor cells with consequent release of tumor-associated neoantigens. Moreover, Wang et al (2017) demonstrated that the use of STING agonist can reverse the resistance to anti PD-1 treatment in mouse models. The lack of cGAS renders mice unable to initiate a beneficial antitumor response when treating with anti PD-L1 inhibitors. This phenotype is reversed by exogenously introducing cGAMP suggesting that the activation of STING is a fundamental step for the successful outcome of the therapies with the immune

checkpoint inhibitors (CKI) (Wang 2017). These evidences enlighten that a combinational therapy with STING agonists and CKI could result in a more beneficial outcome compared to the single treatments.

The first therapeutic approach in the pharmacological activation of STING was accomplished by developing synthetic analogues of 2',3'-cGAMP. In mouse models of colorectal cancer and melanoma, intra-tumoral injection of cGAMP trigger the tumoral antigen presentation by dendritic cells to activate T cell response (Demaria 2015). However, the significant differences between the human and murine STING protein, is an essential parameter to consider. The first STING agonist designed 5,6-Dimethylxanthenone-4-acetic Acid (DMXAA) displayed a very promising outcome in mouse models whereas completely failed in human clinical trials (Shish 2018).

Currently, there are two clinical trial ongoing of STING agonists (ADU-S100 and MK-1454) for the treatment of solid tumors. Preliminary data demonstrate that both ADU-S100 and MK-1454 display a CD8+ tumor infiltration in the injection site (Harrington 2018, Meric-Bernstam 2019). However, because of their efficacy is dependent on the intratumoral inoculation their use might be limited for the treatment of accessible tumors. Aminobenzimidazole, a recently developed STING agonist, has been found to induce CD8+ antitumor immunity. Due to its intravenous delivery and its fast clearance, it has been described to be able to priming STING without prolonged exposure that can result in undesired effects (Ramanjulu 2018).

The use of STING agonists has been proposed also in chronic viral and bacterial infection and as a vaccine adjuvant. CDNs used as adjuvant improve the efficacy of vaccination improving antigen-specific IgG response (Van Dis 2018, Blaauboer 2014, Martin 2017).

On the opposite, the inhibition of STING is a very promising therapy for the treatment of autoinflammatory disease as AGS and SAVI. With a large screening of chemical compounds, Haag et al (2018) identified C-170 and C-171 two

nitrofuran derivate able to negative regulate STING in vitro. The compounds function by inhibiting the palmitoylation and the consequent translocation to Golgi. This result in reduced expression of IL-1β, TNF-α and IL-6. The mechanism of action of these compounds seems to be related to AMPK since its inhibition reverted the phenotype (Peng 2020).

1.11 STING in COVID-19 infections

The 2019 pandemic which spread worldwide in few months has aroused the interest around the master regulators of the immune response in order to counteract the infection by SARS-CoV-2. Among these proteins, an important role of STING in counteracting the viral infection has been hypothesized. These hypotheses are sustained by a series of clues that render STING a possible junction point in the inhibition of the viral replication. First, the similarity of symptomatology of COVID-19 and SAVI both related to an excessive IFN-response signature with fever, pulmonary inflammation with interstitial lung disease, lymphopenia and inflammatory vasculopathy would fit with the possibility that delayed STING overstimulation could be one of the causes (Liu 2014). The age associated severity of COVID-19 could also be connected with the overload of STING signaling in aging, metabolic disorders, diabetes and obesity (West 2015).

Another supporting evidence is found by analyzing the evolutionary differences in STING. Bats, which have been described as the first carrying organism of SARS-CoV2, display a mutation in the STING protein precisely at the phosphorylation site at Ser358. This substitution is associated with a less expression of IFN-β. The high level of DNA damage triggered by high metabolic demand of flight could explicate the reason why during the evolution bats have positively selected this mutation. Probably, this substitution dampens the

induction of STING in bats to avoid an excess of its activation so explaining their high capacity of coexist with viruses (). Finally, another member of Betacoronaviruses, Sars-CoV was previously described to interact with STING through several viral papain-like protease (Xie 2018).

Taken together all these evidences has pushed the scientific community to investigate a possible correlation between STING and SARS-CoV-2 infection. Particularly two recent works has clearly demonstrated the fair assumption of correlation between STING and SARS-CoV2. Rui et al demonstrated that a via the ORF3A, both SARS-COV and SARS-CoV-2 inhibit the activation of cGAS-STING axis. In particular the inhibition affects the activation of Nf-κB without interfere with IRF3 (Rui 2021).

Moreover, Liu et al (2021) demonstrated that the treatment with STING agonist is able to dampen the infectious ability of the virus both cell lines and lung tissues slides. In particular, in contrast with the previous study, the effect of STING agonist on dampening SARS-CoC-2 infection seems to rely upon triggering of IRF3. When IRF3 is deleted, STING agonist is no longer capable of inhibit the infection (Liu 2021).

1.12 The mechanisms of antigen presentation

Besides the immediate response generated by innate immunity at the beginning of the infection, other mechanisms are needed to trigger adaptive response T-lymphocytes dependent. The connection between innate and adaptive immunity is mediated by Major Histocompatibility Complex (MHC). The loading of small peptides (antigens) on the MHC complex is a fundamental prerequisite to generate a specific response against the pathogen (Blum 2013). Depending on the origin of the antigen, the induction of adaptive immunity may occur via two types of MHC complexes. The MHC class I (MHC-I) is expressed by all cells

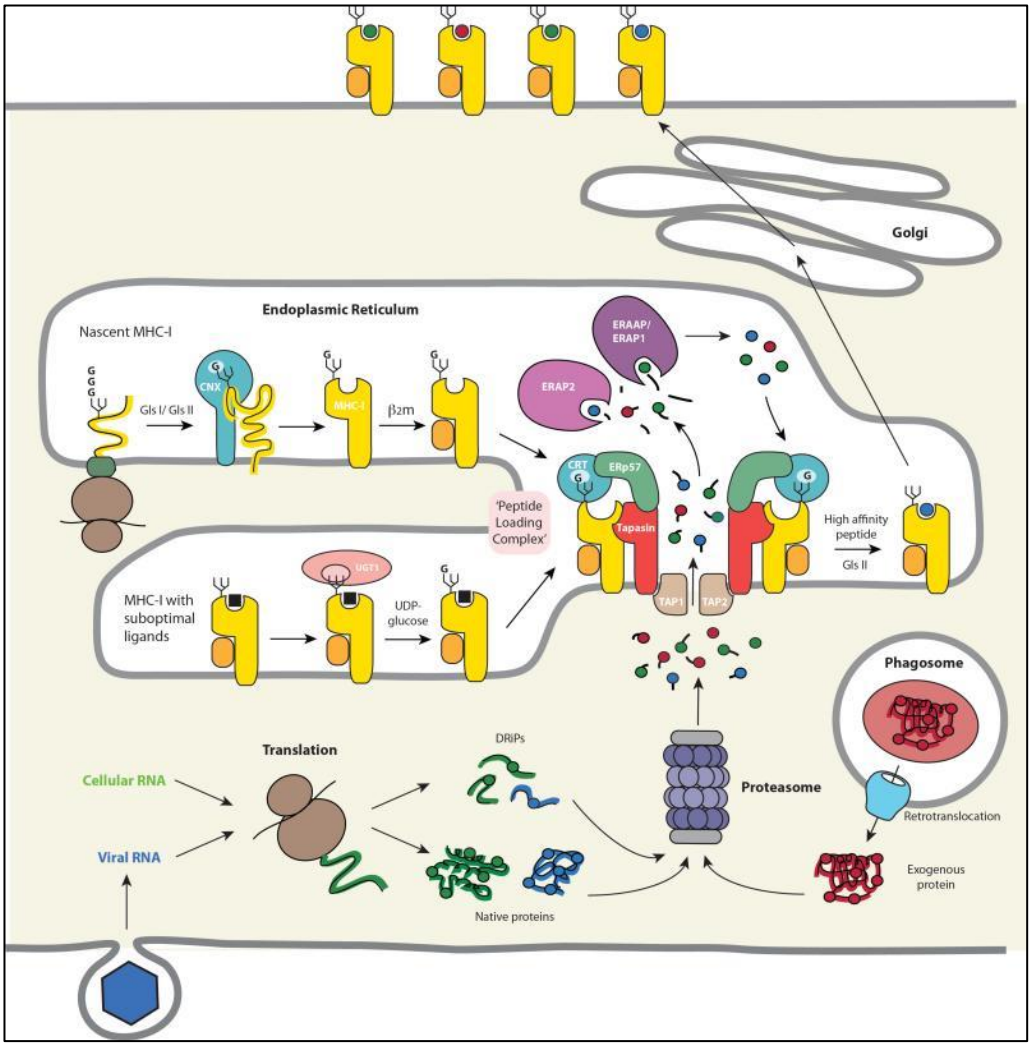

Fig.4 MHC-I-dependent antigen presentation. (Blum 2013)

and represent a "kill me" signal that activate the T-CD8$^+$ cytotoxic response. Antigens loaded on MHC-I originate from cytoplasm and derive from pathogens that have infected the cell or neoantigens produced by the tumor. Only professional antigen presenting cells (APCs) comprehending dendritic cells, phagocytes and B lymphocytes, express the MHC class II (MHC-II) complex which activate the CD4$^+$ T-cell response. Upon processing via endosomal signaling some antigens may escape the endosome, enter the ER and associate with MHC-I in a process named cross-priming (Blum 2013).

The MHC-I complex is composed by a heavy chain (H2 -K, -L and -D in mouse and HLA -A, -B and -C in human) and a β2-microglobulin (β2m) light chain (Adams 2013). Proteasome dependent proteolysis generate short peptides (8-10 amino acids) that are transported in the ER and loaded on MHC-I (Fig. 4). This process is regulated by a multi-protein complex named peptide loading complex (PLC) (Adams 2013). The transport into the ER is mediated by the Transporter associated Antigen Processing (TAP) proteins. TAP is a heterodimeric complex formed by TAP1 and TAP2 (Oancea 2009). Tapasin (or TAP binding protein, TAPBP), functions as a link between the TAP complex and MHC-I chain. Particularly, TAPBP maintain MHC-I complex on the ER membrane so allowing the loading of the antigen (Ortmann 1997). Other proteins, as Calnexin (CLX), Calreticulin (CLR) and protein disulfide-isomerase A3 (ERp57) function as chaperons in mediating the quality control of the process (Hebert 2005). If the peptide entering the ER is longer than 10 amino acids the ER aminopeptidase ERAP1 and ERAP2 generate the antigen of the correct size (Saveanu 2005).

The MHC-II presentation begin with the internalization of an exogenous antigen via endocytic signaling. The antigen is proteolyzed in the vesicles by Cathepsins to generate fragments of 13-25 amino acids (Blum 2013). MHC-II complex is composed by α and β subunits which assembles to form the mature form (I-A and I-E in mouse, HLA-DR, HLA-DQ and HLA-DP in human). The complex is assembled within the ER and the process is mediated by a specific chaperon, the invariant chain (Ii chain). Beside facilitating the interaction between α and β chains, Ii blocks MHC-II peptide binding cleft in order to avoid the interaction with non-specific antigens (Landsverk 2009). Following its assembly, MHC-II is matured in endosomal compartment where cathepsins mediate the cleavage of Ii in a smaller protein, CLIP. Upon CLIP removal by HLA-DM the MHC-II complex is able to bind the antigen and migrate on the cell surface (Landsverk 2009).

2. Aim

Recent accumulating evidence have enlightened that the initial role identified for the STING protein in simply attend the IFNs-dependent innate immune response were quite underestimate its potential. Since its discovery in 2008, and the canonical role that has been described, STING has been found to function in a broad range of physiological and pathological processing. It has been connected with the pathogenesis of autoimmune disorders (SAVI), the induction of apoptosis via MHC-II signalling and autophagy vesicles formation. Most recently it has been demonstrated its implication in cancer development despite the exact mechanism of action still remain controversial. In particular, it seems to have a central role in the cross-presentation of tumoral neoantigen for the activation of T-lymphocytes antitumoral immunity. Indeed, treatment of mouse models with STING agonists have displayed an amelioration of the symptomatology connected to the induction on T-cell antitumor immunity.

During my PhD fellow I focused my attention on the evaluation of the role of STING in immune response by analysing its implication in the antigen presentation. To this purpose I generated mouse and human STING KO cell lines to evaluate the differences in antigen presentation. To this purpose I evaluated the differences in the cell surface expression of the OVA-derived SIINFEKL antigen through FACS analysis. Moreover, I investigated on the regulation of the molecular mechanism related. Aside from the analysis of PLC complex both at mRNA and protein levels I focused on STAT1 and Nf-κB signalling which are described as major regulators of immune response. The different behaviour of STING KO cells upon treatment with OVA was also observed after LPS treatment in both human and mouse cell lines. Finally, an analysis of plasma membrane receptors expression displayed a different pattern in absence of STING.

Materials and Methods

3.1 Chemicals

Chemicals were purchased from the following manufacturers: Dulbecco's modified Eagle's medium (DMEM), RPMI 1640, fetal bovine serum (FBS), penicillin-streptomycin, phosphate buffer saline (PBS), Trypsin-EDTA 0.25% and IFN-γ from GIBCO (Thermo Fisher Scientific, Inc., Waltham, MA, USA); protease and phosphatase inhibitors cocktails from Roche Diagnostic (Meylan, France); Protein assay, Acrylamide/Bis-acrylamide solution 40% from Bio-rad (Munchen, Germany), ECL from Elabscience (Houston, TX, USA); Pageruler^{TM} Protein Ladder, Alexa Fluor^{TM} 488-conjugated ovalbumin, DQ-ovalbumin and ProLongTM Gold Antifade Mountant with DAPI from Invitrogen-Thermo Fisher Scientific; Formaldehyde solution 37%, Glycine, Ovalbumin (OVA) and Lipopolysaccharides (LPS) from Sigma-Aldrich (St. Luis, MI, USA).

3.2 Antibodies

The following antibodies were purchased: rabbit polyclonal anti STING #19851-a-AP (Proteintech, Rosemont, IL, USA), mouse monoclonal anti p-STAT1 (Y701) sc-136229 (Santa Cruz Biotechnology, Dallas, TX, USA), mouse polyclonal anti-STAT1 A302-753A (Bethyl Laboratories Inc., Montgomery, TX, USA), mouse monoclonal anti TAP1 (D-11) sc-518133 (Santacruz Biotechnology), mouse monoclonal anti TAP2 (B-2) sc-515576 (Santacruz Biotechnology), mouse monoclonal anti TAPBP (TO-3) (Santacruz Biotechnology), mouse monoclonal anti γ-tubulin #T6657 (Sigma-Aldrich, St.

Louis, MI, USA), rabbit polyclonal anti p-65 #06418 (Sigma-Aldrich), rabbit monoclonal anti RelB (C1E4) #4922 (Cell Signaling Technology, Danvers, MA, USA), rabbit polyclonal anti c-rel sc-71 (Santacruz Biotechnology), mouse monoclonal GAPDH (0411) sc-32233 (Santacruz Biotechnology), rabbit polyclonal anti IκB-α sc-371 (Santacruz Biotechnology), rabbit monoclonal anti Histone H3 (3H1) #9717 (Cell Signaling Technology), FITC mouse monoclonal CD11b (M1/70) #01714D (BD PharMingen, San Diego, CA, USA), FITC mouse monoclonal CD11c (HL3) #55381 (BD PharMingen), FITC mouse monoclonal CD86 (B7-2) #09274D (BD PharMingen), FITC mouse monoclonal MHC Class I (H-2Kb) (AF6-88.5.5.3) #11-5958-83 (eBioscience™-Thermo Fisher Scientific), PE mouse monoclonal SIINFEKL/H-2Kb (eBio25-D1.16) and horseradish peroxidase (HRP)-conjugated secondary antibodies GtxRb-003-DHRPX and GtxMu-003-DHRPX (Immuno Reagents Inc., Raleigh, NC).

3.3 Design and cloning of gRNAs

Genomic sequence of both mouse and human TMEM173 were analysed in order to identify the target regions for Cas9 double strand break. Mouse TMEM173 is located on reverse strand of chromosome 18 whereas human TMEM173 is located on reverse strand of chromosome 5. Both of them are composed by 8 Exons (6 coding). Guide RNAs are designed to target the first codifying exon both in mouse and in human. Murine gRNAs target exon 3 (gRNA1 and 2) and exon 4 (gRNA3) while exon 3 of human TMEM173 contains both human gRNAs. Guide RNAs were designed by using an online tool (http//:www.zlab.bio/guide-design-resources). For knocking out mouse STING, three gRNAs were designed whereas human STING was targeted by 2. The target sequences are displayed below.

	Target sequence	Direction	PAM
M gRNA1	CACCTAGCCTCGCACGAACT	FW	TGG
M gRNA2	GAGGTCACCGCTCCAAATAT	REV	TGG
M gRNA3	GGGATGCCCCATCCACTGTA	FW	TGG
H gRNA1	GTGACCCCTGGGACACGGGA	REV	TGG
H gRNA2	GCTGGGACTGCTGTTAAAC	FW	GGG

Guide RNAs were purchased as single stranded primers from Eurofins Genomics (Ebersberg, Munich, DE) as follow:

Mouse gRNA1 fw: 5'- CACCGCACCTAGCCTCGCACGAACT -3'

Mouse gRNA1 rev: 5'- AAACAGTTCGTGCGAGGCTAGGTGC -3'

Mouse gRNA2 fw: 5'- CACCGATATTTGGAGCGGTGACCTC -3'

Mouse gRNA2 rev: 5'- AAACGAGGTCACCGCTCCAAATATC -3'

Mouse gRNA3 fw: 5'- CACCGGGGATGCCCCATCCACTGTA -3'

Mouse gRNA3 rev: 5'- AAACTACAGTGGATGGGGCATCCCC -3'

Human gRNA1 fw: 5'- CACCGGTGACCCCTGGGACACGGGA -3'

Human gRNA1 rev: 5'- AAACTCCCGTGTCCCAGGGGTCACC -3'

Human gRNA2 fw: 5'- CACCGGCTCGGACTGCTGTTAAAC -3'

Human gRNA2 rev: 5'- AAACGTTTAACAGCAGTCCCAGCC -3'

Double stranded DNA fragments were obtained by preparing a mixture containing: 10 μM primer fw, 10 μM primer rev, 50 mM Tris-HCl, 10 mM $MgCl_2$, 10 mM Dithiothreitol, 1 mM ATP. The mixture was incubated for 30 min at 37 °C following by 5 min at 95°C and slowly cooled down to room

temperature. Double stranded gRNAs were digested with BbsI and cloned into px458 (Addgene) kindly provided by prof. Silvia Parisi (University of Naples).

3.4 Cell cultures

J774, kindly provided by prof. Maurizio Renna, were cultured in DMEM supplemented with 10% FBS, 2mM glutamine and 0.5 mg/ml of pen-strep. CT26, kindly provided by Nouscom srl, U937, kindly provided by prof. Michela Grosso's lab and THP-1, kindly provided by prof. Francesca Calromagno's lab, were cultured in RPMI 1640 medium supplemented with 10% FBS, 2 mM glutamine and 0.5 mg/ml of pen-strep. All the cultures were maintained in a humidified incubator at 37°C with 5% CO_2.

Antigen presentation assay was performed by incubating cells in full medium with 0.5 μg/μl for 24h. As negative control, cells were treated with the same volume of PBS.

For LPS treatments, cells were incubated with 1μg/ml for the indicated time. An equal time course treatment was carried out with DMSO as negative control.

3.5 Generation of STING KO clones

J774 were transduced with DNA by nucleofection. $1.5x10^6$ cells were centrifuged, washed with PBS and resuspended in 100 μl of nucleofection medium from Cell line nucleofector Kit L (Lonza Group Ltd, Basel, Switzerland) with 3 μg of plasmids expressing the gRNAs (1 μg each). The mixture was transferred in Nucleocuvettes and U23 setting of Nucleofector™ 2b

(Lonza) was used for the transduction. Cells were cultured in 6 multiwell (MW) plates in normal growth condition for 48h. Single clones were selected by limiting diluition in 96 multiwell. KO clones were selected by western blot analysis.

CT26 and U937 were transfected by using Lipofectamine 2000 (Invitrogen, Thermo Fisher Scientific, Inc.,) according to the manufacturer's protocol.

THP-1 cells were transduced with lentiviral particles derived by LenticrispV2. Following transfection or infection CT26, U937 and THP-1 were subjected to limited dilution and single clones were selected as described previously.

3.6 Western blot analysis

Cells were lysed in RIPA Buffer (150 mM NaCl, 2% NP40, 0.1% SDS, 50 mM Tris HCl) supplemented with protease and phosphatase inhibitors on ice for 30 min. Upon centrifugation protein concentrations were evaluated by Bio-rad assay. 30 μg of proteins were resuspended in Laemmli buffer (4% SDS, 10% β- mercaptoethanol, 20% glycerol, 0,125 M Tris HCl, 0.004% bromphenol blue) and resolved by SDS-PAGE. Proteins were transferred on Immobilon-P PVDF membrane (Merck-Millipore, Burlington, MA, USA) and membranes were blocked in 5% non-fat milk (neoFroxx GmbH, Einhausen, Germany). Membranes were immunoblotted overnight with primary antibodies at 4 °C following three washing with TBS. Incubation with secondary antibody was performed for 1h at room temperature. After three washes with TBS Tween20 (0.1%) enhanced chemiluminescence (ECL) was used for protein detection. Image-J software was used for the densitometric analysis.

3.7 Nuclear/cytosol fractionations

Cells were lysed in Buffer B (10 mM Hepes, 1.5 mM $MgCl_2$, 10 mM KCl, 0.5 mM DTT, 0.1 % NP40) supplemented with protease and phosphatase inhibitors on ice for 5 min. Upon centrifugation cytosolic protein extracts were collected and upon 3 washes in Buffer A (10 mM Hepes, 1.5 mM $MgCl_2$, 10 mM KCl, 0.5 mM DTT), nuclei were lysed in Buffer C (20 mM Hepes, 25% Glycerol, 0.42 M NaCl, 1.5 mM $MgCl_2$, 0.2 mM EDTA, 0.5 mM PMSF, 0.5 mM DTT) for 30 min on ice followed by 3 cycles of freeze and thaw. Upon centrifugation, nuclear extracts were collected.

3.8 Co-immunoprecipitation (Co-IP) assay

Cells were lysed in RIPA buffer containing protease and phosphatase inhibitors for 30 min on ice. After centrifugation 1 μg of whole cell lysates was pre-cleared for 1 h at 4 °C with rotation. 1 μg of rabbit anti-STING was incubated with 30 μl of Protein-A Sepharose (GE Healthcare, Chicago, IL, USA) for 1h at 4 °C with rotation. Pre-cleared lysates were then incubated with the mixture of Protein-A-anti-STING and kept in rotation at 4 °C overnight. Following three washes in RIPA buffer, samples were then separated by SDS-page as described above.

3.9 Uptake and proteolysis assay

J774 and J774 STING KO were seeded at $5x10^4$ cells on 0.22mm glass coverslip in 12 MW and incubated overnight in standard culture conditions.

For the uptake assay, cells were washed three times with PBS 1x and then incubated for 30 min with 50 μg/ml of Alexa Fluor™ 488-conjugated ovalbumin (Thermo Fisher Scientific) in serum free DMEM at 37 °C. Negative controls were performed on ice as above. Cells were washed three times with PBS, fixed and processed for immunofluorescence.

Proteolysis assay was performed in serum free DMEM. Cells were washed three times with PBS and pulsed for 3 min with 50 μg/ml of DQ-ovalbumin (Thermo Fisher Scientific). Following three washes with PBS cells were incubated in serum free medium for 30 min at 37°C. Negative controls were carried out on ice as above. After incubation, cells were washed three times with PBS, fixed and processed for immunofluorescence.

3.10 Fluorescence microscopy

Cells were seeded at $5x10^4$ on glass coverslips and incubated overnight in standard growth condition. The next day, cells were rinsed three time with PBS and fixed in 3.7% formaldehyde for 30 min at room temperature. Formaldehyde quenching was performed by 10 min of room temperature incubation with glycine 0.1 M. Cells were permeabilized by incubation with blocking buffer (1% BSA, 0.01% Sodium Azide and 0.02% saponin in PBS) for 10 min at room temperature. Immunostaining was carried out at room temperature for 1h. Following three washes with PBS, cells were incubated with secondary antibodies for 30 min at room temperature. Finally, coverslips were rinsed with distilled water and mounted onto glass slides with the Prolong Gold anti-fade reagent with DAPI (Invitrogen, Thermo Fisher Scientific). Images were collected by using a laser scanning microscope (LEICA DMi8) and analyzed using LEICA LAS X software.

3.11 Flow Cytometry

Cells were detached from the plate with cell detachment buffer (PBS 1x, EDTA 0.5 M) and labeled with primary antibody for 30 min at 4 °C in the dark. Following three washes with PBS, cells were analyzed with BD Accuri™ C6 cytometer (BD Biosciences, San Jose, CA, USA). A relative Ig isotype antibody was used as control of non-specific binding. Data were collected by using BD Accuri C6 software (BD Biosciences).

3.12 Real-Time PCR

Total RNA was extracted using TRIzol reagent (Invitrogen) as manufacturer's instructions. 1 μg of RNA was used for cDNA synthesis with M-Mulv Reverse Transcriptase (New England Biolabs Ipswich, MA, USA). The reaction was carried out as following: 25 °C for 5 min, 42 °C for 1h, 65 °C for 20 min. Real-Time PCR was performed by using SensiFAST™ Sybr Green (Bioline, Meridian Bioscience, Cincinnati, OH, USA) with QuantStudio™ 7 (Applied Biosystem). Reactions was run in triplicate in at least three independent experiments. Target expressions were normalized against the housekeeper gene GAPDH and analyzed with $2^{-\Delta\Delta CT}$ method (Livak and Schmittgen 2001). Fold changes in gene expression were normalized to an internal control (J774 NT). Primer-BLAST tool (https://www.ncbi.nlm.nih.gov/tools/primer-blast/) was used for the design of primers which were purchased by Eurofins Genomics. The following primers were used to amplify the target genes:

STAT1 fw:	5’- GTTCCGACACCTGCAACTGAA -3’
STAT1 rev:	5’- ACGACAGGAAGAGAGGTGGT -3’
H2K1 fw:	5’- CAGGTGGAAAAGGAGGGGAC -3’
H2K1 rev:	5’- CTGAGGGCTCTGGATGTCAC -3’
β2m fw:	5’- GACCGGCCTGTATGCTATCC -3’
β2m rev:	5’- TGTCTCGATCCCAGTAGACG -3’
CD11c fw:	5’- GGCTGCAAGCATCATTCGTT -3’
CD11c rev:	5’- TTGGTGTCTCTGTGCCCTC -3’
TAP1 fw:	5’- GGCTTACGTGGCTGAAGTCT -3’
TAP1 rev:	5’- GAGAGCAGGACCTGAACAGC -3’
TAP2 fw:	5’- GCAGACGACTTCATAGGGGAA -3’
TAP2 rev:	5’- TCTGTAGGGCCTGTTCACAC -3’
TAPBP fw:	5’- TGGCTGGTAGCTGCCTACT -3’
TAPBP rev:	5’- TGGCTTCCACAGACGAGAAC -3’

The array analysis of Nf-κB downstream genes was performed with RT2 Profiler PCR Assays (PAMM-025Z) (Qiagen, Hilden, Germany).

3.13 Statistical analysis

Data analysis derives by at least three independent experiments. Statistics was performed by Student’s *t*-test with significant p-value threshold <0.05.

4 Results

4.1 Design of experimental model

In order to evaluate the role of STING in MHCI related antigen presentation we generated a STING KO J774 murine macrophages cell line by using the CRISPR/Cas9 system. Guide RNAs were designed to target exon 3 and exon 4 of mouse TMEM173 gene as showed in Fig. 5A. The guide RNAs were cloned in the Cas9 expression vector px458. The experimental procedure is summarized in Fig.5B. Transduction of exogenous DNA was accomplished by using nucleofection. Following limiting dilution, a single clone derived J774 STING KO cell line was obtained (Fig.5C).

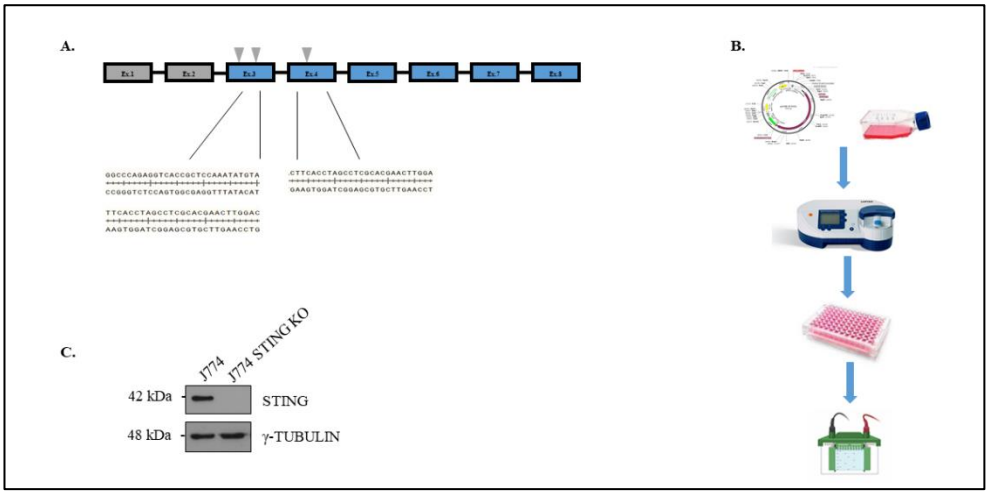

Fig 5. Schematic resuming of STING KO generation.

A. Graphic representation of TMEM173 gene. The ATG is located in the third exon, thus gRNAs are designed to target exon 3 and exon 4. B. Workflow of STING KO J774 generation. C. Western blot analysis of STING protein in J774 and its KO counterpart. γ-tubulin was used as standard.

4.2 The lack of STING impairs the antigen presentation

An approach frequently used for the studies on the antigen presentation relies on chicken ovalbumin (OVA) assay. By mimicking an infection from an exogenous host, OVA is internalized into the cells and processed in a pathogen-like response. Once in the cytosol, ovalbumin can undergo to a dual fate. It can be processed via endosomal vesicles in order to be associated to MHC class II for triggering $CD4^+$ T-cells. On the other hand, it can be proteolyzed via proteasome in order to generate epitopes that enter the endoplasmic reticulum and associate with MHC class I resulting in $CD8^+$ lymphocytes activation. The

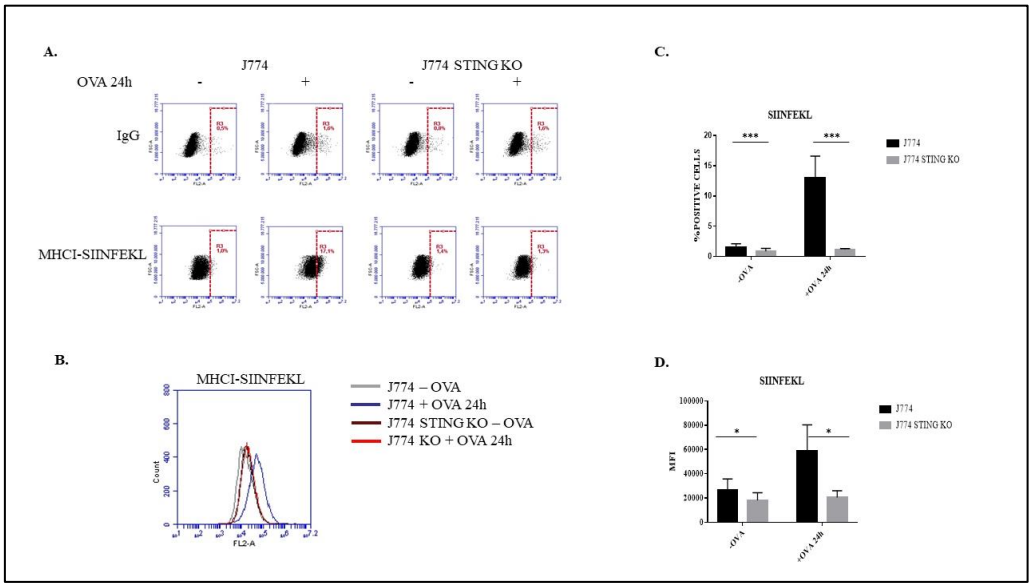

Fig 6. STING KO macrophages are unable to present SIINFEKL peptide on plasma membrane.

FACS analysis of SIINFEKL peptide in WT and STING KO as plots (A) or histograms (B); a relative Ig isotype antibody was used as control of non-specific binding. Upon OVA treatment ~15% of WT cells present the SIINFEKL peptide on plasma membrane (C) with increasing of MFI (D)

whereas no signal was found in KO. Data are representative of three independent experiments.

assay is based on the generation, upon OVA proteolysis, of a specific epitope named SIINFEKL (Ser, Ile, Ile, Asn, Phe, Glu, Lys, Leu).

J774, as macrophages cell line, are able to mimic both these responses and represent a perfect in vitro model to study both mechanisms. Here we analyze the MHC-I related OVA presentation.

J774 and J774 STING KO were incubated with OVA or PBS as negative control for 24h. The detection of SIINFEKL presentation occurs via a phycoerythrin (PE)-conjugated antibody raised against the complex MHC-I-SIINFEKL. After incubation we observed a 17.1% of SIINFEKL presenting cells in WT whereas no positivity was detected in J774 STING KO (Fig. 6A and B). As expected not all WT cells resulted positive for the detection of the complex since the antibody recognition can occur only in the presence of SIINFEKL so excluding all the other epitopes generated by the OVA proteolysis. The analysis of the number of positive cells (Fig. 6C) and MFI (Fig. 6D) revealed a significative difference between J774 and J774 STING KO.

4.3 The impairment of antigen presentation does not rely upon entry and proteolysis of exogenous proteins

Following the observation of antigen presentation impairment in the STING KO J774, we attempted to identify the stage involved in the process.

The first step we focused on was the ability of internalizing the exogenous host. To accomplish this, we evaluated whether the uptake of OVA was impaired between WT and KO by using a modified Alexa 488-ovalbumin

(OVA-A488). J774 and J774 STING KO were incubated with OVA-A488 for 30 min at 37 °C.

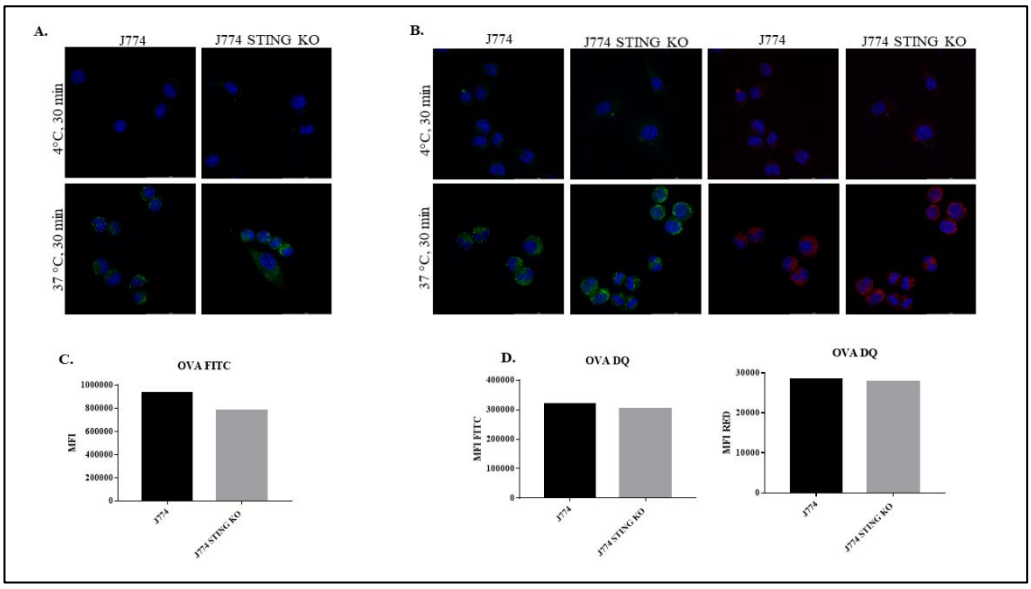

Fig 7. The Uptake and proteolysis of OVA are not impaired in STING KO.

A. J774 and J774 STING KO were incubated with 50 μg/ml of Alexa 488-conjugated ovalbumin for 30 min at 37 °C or on ice and then fixed in 4% paraformaldehyde. Ovalbumin was equally internalized in WT and KO (C).
B. WT and KO J774 were pulsed with 50 μg/ml of DQ-ovalbumin for 3 min and chased for 30 min at 37 °C. Continuous incubation on ice was performed as negative control. No differences in OVA proteolysis were observed (D).

Negative control was performed as above on ice. As expected, when the cells were incubated on ice the internalization of OVA was prevented. However, after 30 minutes at 37 °C ovalbumin was correctly internalised into the cells without any detectable differences between WT and KO (Fig. 7A and C).

We moved further to explore the possible impairment of the proteolytic activity by the use of DQ-ovalbumin (DQ-OVA). DQ-OVA has a dual role in

investigating on both MHC-I and MHC-II related antigen presentation. It is a self-quenched conjugate of ovalbumin that express fluorescence at 515 nm upon proteolytic degradation. Moreover, when digested fragments accumulate in endosomal compartments, they aggregate into excimers that can be visualized by using a red-light long pass filter. Because of the localization of excimers, the red fluorescence is indicative of proteolysis occurring during MHC-II related antigen processing. Both J774 and J774 STING KO were pulsed with DQ-ovalbumin for 3 min following by 30 min of chase at 37°C. The same treatment was performed on ice to block internalization and proteolysis (Fig. 7B upper panels). After 30 min of DQ-OVA treatment at 37 °C both WT and KO cells displayed a green fluorescence into the cytosol indicative of a correct proteolysis (Fig. 7B lower panels). Moreover, the same pattern was found in the red spectrum suggesting that, if the defect in MHC-I mirrors an impairment of MHC-II presentation, it does not rely upon a dampened proteolysis in endosomal compartments (Fig. 7B and D).

4.4 Evaluation of STING involvement in peptide loading

Once excluded the uptake and the proteolysis we focused on the peptide loading on MHC-I. Following treatment for 24h with OVA J774 and J774 STING KO were analyzed by immunofluorescence against MHC-I-SIINFEKL complex. In contrast to the previously conducted analysis, in this experiment the cells were permeabilized in order to visualize the intracellular complex. Cells treated with PBS, as negative control, are shown in fig. 8 upper panel. Upon OVA treatment, J774 displayed an accumulation of dots corresponding to MHC-I-OVA complexes whereas in STING KO this pattern was not found (Fig. 8 lower panel). This encouraged us to further investigate on the peptide loading on MHC-I. Since the peptide loading complex (PLC), composed by TAP1, TAP2 and

TAPBP, is important in antigen presentation, we explored whether the expression of these proteins correlate with STING expression. WT and KO cells

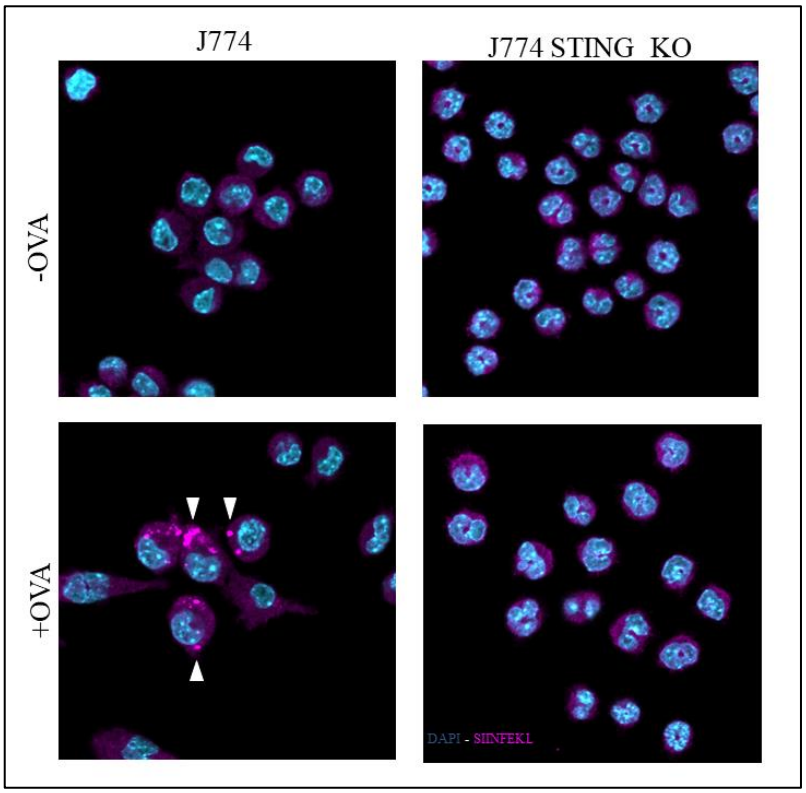

Fig 8. Peptide loading complex was impaired in STING KO.

J774 WT and KO were treated with ovalbumin for 24h, cells were fixed in 4% paraformaldehyde and analysed for MHC-I SIINFEKL intracellular localization. In KO cells, the OVA treatment did not induce the formation of MHC-I-SIINFEKL complexes (indicated by arrows).

were treated with OVA and total mRNAs were collected at different time points. Surprisingly, the analysis of TAPs transcriptional levels displayed a significative difference yet at basal level with an impressive decrease of TAP1, TAP2 and TAPBP in STING KO (Fig. 9A). Moreover, their expression was induced by OVA treatment with peaking at 4h of treatment (Fig. 9A black bars). In STING

KO, however, the positive regulation of OVA on the expression of these proteins failed (Fig. 9A gray bars). However, this difference in expression was not observed by analyzing the protein levels (Fig. 9B and C). The next step was to evaluate whether STING could participate in the assembly of the peptide loading complex. J774 were treated with OVA for 4h and 24h and co-immunoprecipitation assay was conducted by pulling down STING. The SDS page derived revealed no interaction between STING and TAP1 during OVA treatment (Fig. 9D).

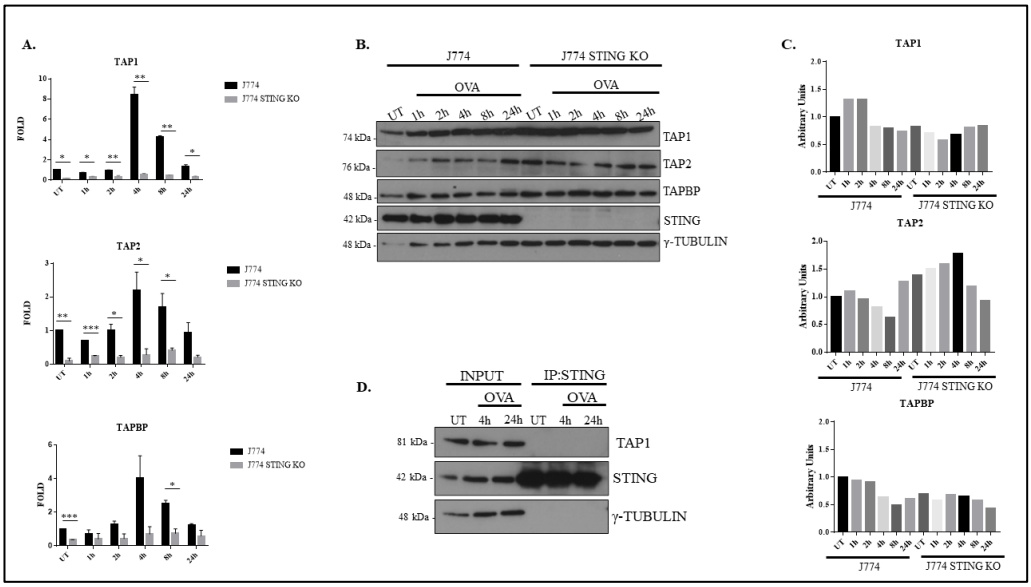

Fig 9. The PLC protein expression was not impaired in STING KO macrophages.

A. Gene expression analysis displayed a marked reduced level of TAP1, TAP2 and TAPBP in STING KO at steady state. The OVA-induced increase at 4h was absent in STING KO (grey bars). B. Western blot analysis of TAP1, TAP2 and TAPBP protein expression levels. C. The densitometric analysis display no differences between WT and KO. D. J774 macrophages were treated with OVA for the indicated time. Co-IP revealed no interaction between STING and TAP1.

4.5 Membrane localization of MHC-I is dampened in STING KO

We further investigated on MHC-I complex by analyzing mRNA levels and the cell surface localization of the protein. Cells were treated with OVA for 24h and stained with anti MHC-I FITC antibody while IgG staining was performed as negative control. The cytofluorimetric analysis displayed a very drastic difference between J774 WT and J774 STING KO (Fig. 10A, B and C). The J774 WT displayed 80% of MHC-I positive cells at steady state with increasing at 98.5% after 24h of treatment with OVA (Fig. 10A, B and C). In contrast, in the J774 STING KO the basal level of MHC-I on the cell surface was deeply compromised (8.7%) and there was a slight increase after 24h of treatment with OVA (30.5%). Thus, MHC-I expression on plasma membrane was still inducible by OVA in the KO cells yet the gap with the WT was not rescued. Based on these results, we further evaluated whether the MHC-I gene expression was reduced in the KO cells. MHC-I complex is composed by a heavy chain (K, D or L) and β_2-microglobulin (β_2m). β_2m is necessary for the association of heavy chain with the complex of peptide loading complex.

Time course of OVA treatment at 1h, 2h, 4h, 8h and 24h was performed on J774 and J774 STING KO in order to evaluate differences in mRNA expression of MHC-I genes. Besides the β_2m, we focused on the analysis of H2K1 since the SIINFEKL assay is restricted to this specific heavy chain. As displayed in fig. 10D, the levels of H2K1 were not divergent between WT and KO neither at steady state or upon OVA treatment. Differently from what we observed with the TAPs, OVA did not induce the expression of MHC-I heavy chain (Fig 10D). Conversely, the analysis of β_2m expression displayed significant differences among WT and KO (Fig. 10E). Basal levels were already dampened in STING KO with a 3-fold decrement compared to the WT cells (Fig. 10E grey bars). Moreover, OVA treatment induced an increase of β_2m gene expression

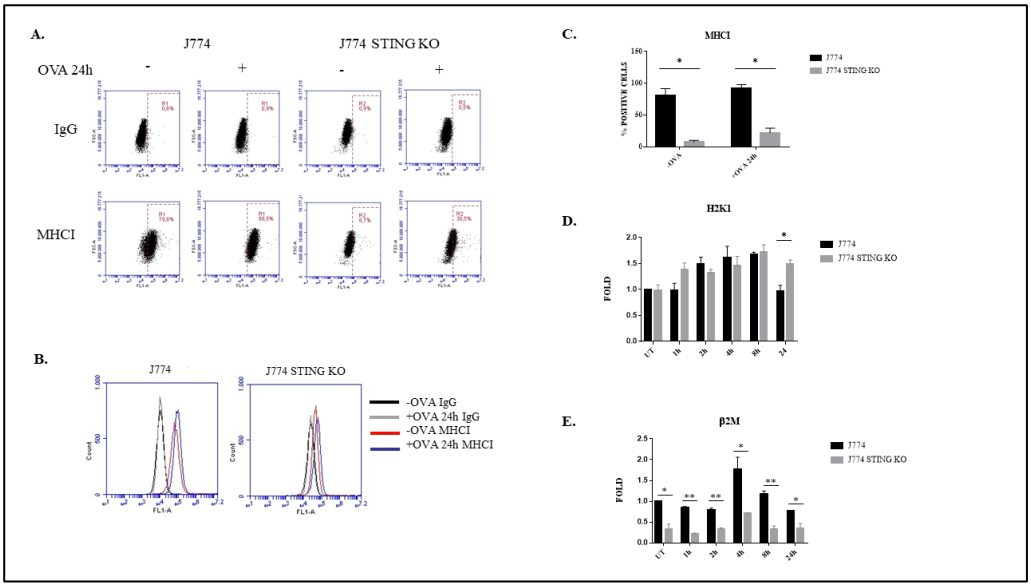

Fig 10. MHC-I cell surface localization is reduced in STING KO.

FACS analysis of MHC-I localization on plasma membrane as plots (A) or histograms (B). WT cells displayed high basal levels of MHC-I complex with a slightly increase upon OVA treatment while, in the KO, the localization was very compromised even upon OVA treatment (C). Relative expression analysis of the H2K1 heavy chain (D) and β2m light chain (E) upon time course OVA treatment. Data are representative of three independent experiments. Student *t* test was used to calculate the statistical significance (* = $p<0.05$, ** = $p<0.01$)

that peaked at 4h. Even though, in the KO β_2m was still induced by OVA, its expression was 2.5-fold decreased compared to the WT.

4.6 OVA-induced STAT1 phosphorylation is compromised in STING KO macrophages

Once assessed that MHC-I expression was dysregulated in STING KO cells we investigated on the possible mechanism that could cause the observed phenotype.

The signalling induced by JAK/STATs is critical for MHC expression both at transcriptional level and on the cell surface. β_2m promoter display sites for ISRE and Nf-κB suggesting that an alteration of these regulatory mechanism could indirectly impair MHC functions. To evaluate whether the reduction of β_2m transcript could be related to a dysregulation of JAK/STAT signaling, we treated WT and KO J774 with OVA in a time course as showed in fig. 11A. As expected, OVA treatment strongly induced STAT1 phosphorylation which peaks at 4h. In contrast, the level of STAT1 phosphorylation was not detectable in KO cells (Fig. 11A). Surprisingly, we found that even the basal level of STAT1 protein was impaired in KO cells with an average of 2-fold decrease. To investigate whether the observed impairment of STAT1 protein expression in the KO cells was depending on gene expression reduction, we analyzed the levels of STAT1 mRNA in WT and KO cells. We noticed the same trend detected in the protein expression (Fig. 11B). Furthermore, in J774 WT, OVA treatment was able to transcriptionally induce STAT1 with a 10-fold increase at 4h which persisted at 8h though at lower levels. The depletion of STING, instead, not only caused a decrease of basal transcription levels, but also impeded the transcriptional activation OVA-induced (Fig. 11B). Taken together these data suggest a fundamental role of STING in regulating both activation and expression of STAT1.

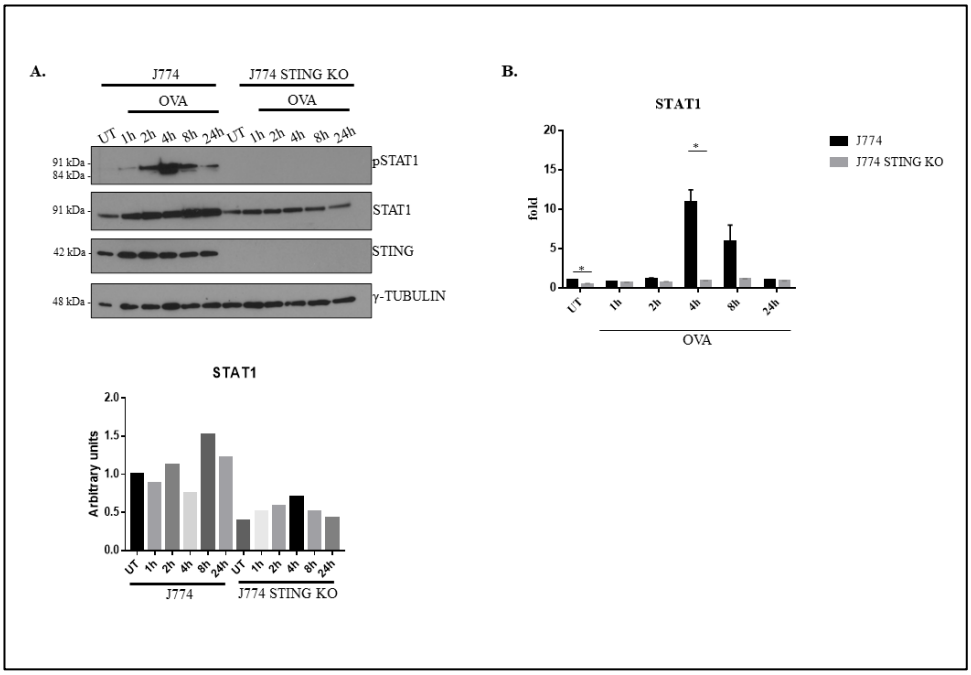

Fig 11. STING KO macrophages failed to trigger OVA-dependent STAT1 phosphorylation.

A. WT and KO J774 were treated with OVA for the indicated times and the phosphorylation of STAT1 in Y701 was evaluated. In WT STAT1 phosphorylation at Y701 peaks at 4h whereas no levels are detected in KO.

B. RT-PCR analysis of STAT1 mRNA expression. Upon OVA treatment STAT1 gene expression was increased at 4h (black bars). No induction was observed in STING KO. Data are representative of 4 independent experiments and statistical significance was evaluated by Student *t* test (* = $p < 0.05$)

4.7 STING KO affects the LPS-induced STAT1 activation

STAT1 activation represent one of the most important hallmarks for the induction of an efficient immune response during infection. It represents a link

between the innate and adaptive immunity and its activation rely upon a very broad range of different stimuli.

To further investigate on the role of STING in triggering STAT1 dependent immune response, we analysed the levels of STAT1 phosphorylation upon LPS treatment. As expected, 4h of LPS treatment induced a strong STAT1 phosphorylation in J774 WT with a decreasing trend towards 24h. Consistent with previous data, no detectable level of phosphorylated STAT1 was observed in J774 STING KO (Fig. 12A).

To investigate whether the role of STING in STAT1 activation occurs in other cellular systems, we evaluated the response to LPS in the CT26 murine colon cancer cell line. CT26 WT and KO were treated as described before. Consistent with previous data, LPS treatment triggered STAT1 phosphorylation at 4h in WT cells whereas no activation was detected in KO (Fig. 12B).

Furthermore, we also investigated whether the role of STING in regulated STAT1 activation is limited to murine system. To address this, we generated STING KO in two human cell lines. U937, a pro-monocytic myeloid leukemia cell line and THP-1 a monocytic cell line were treated with LPS as mentioned above. In the human cell lines, the STAT1 phosphorylation was not completely abolished but still affected in STING KO (Fig. 12C and D). Intriguingly, the decrease of STAT1 protein expression noticed in J774 and CT26 (Fig. 12A and B) was not observed in human cell lines, suggesting an additional mechanism that participates in the regulation of STAT1 protein expression in absence of STING (Fig. 12C and D).

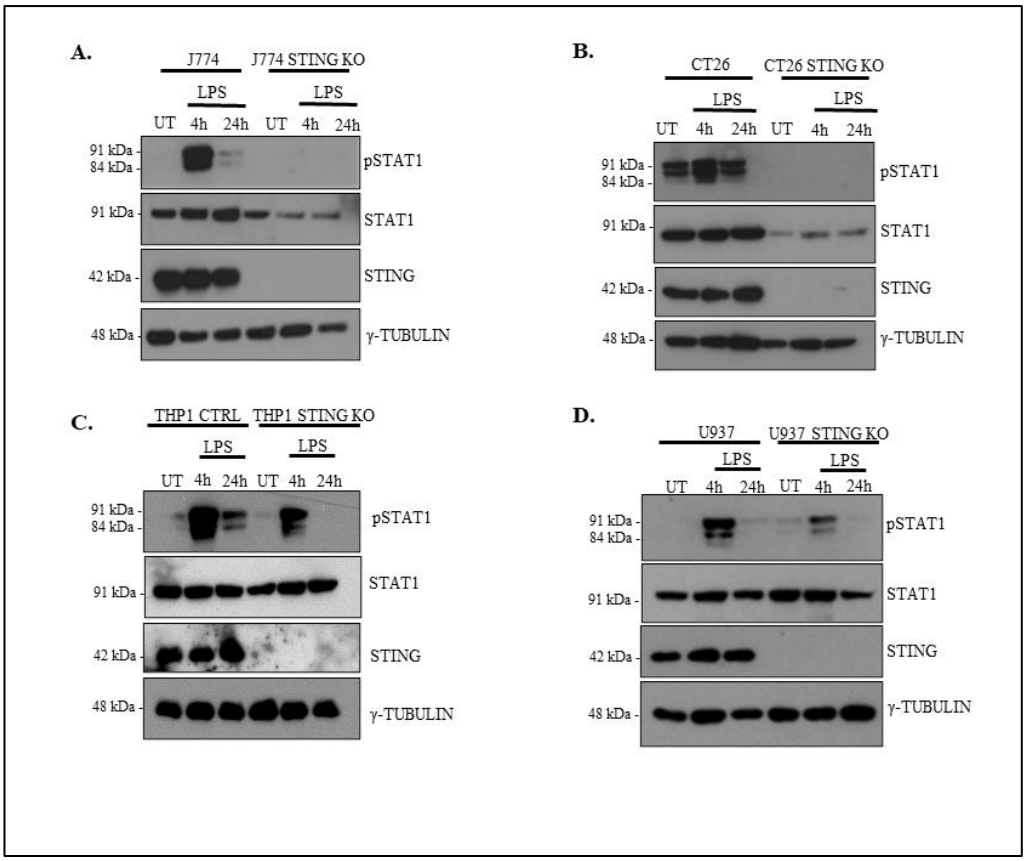

Fig 12. STAT1 phosphorylation was not induced upon LPS treatment in STING KO.

Western blot analysis of LPS treatments at the indicated times in J774 (A), CT26 (B), THP-1 (C) and U937 (D). In STING KO mouse cells (A-B) STAT1 was not phosphorylated upon LPS and basal level of the protein was dampened. In human cell lines (C-D) the STAT1 activation was still induced though to a lesser extent. Data are representative of 4 independent experiments.

4.8 The cell surface localization of CD11c was reduced in STING KO macrophages

The impaired antigen presentation and the reduced MHC-I levels on the plasma membrane encouraged the investigation on a possible role of STING in the regulation of the protein trafficking. To this purpose, we analyzed the cell surface localization of macrophages plasma membrane receptors. CD11b and CD11c belong to integrin family and are involved in adhesion and antigen presentation. CD86 is a receptor that participates to the costimulatory signals essential for T-lymphocyte proliferation.

CD11b trafficking was not impaired as cell surface levels at steady state were not divergent in WT and KO (Fig. 13A). In line with this, neither CD86 was affected by the absence of STING (Fig. 13A). Conversely, CD11c membrane localization was strongly compromised (Fig. 13A). To evaluate whether the defect could be rescued by stimulating the antigen presentation, we treated J774 WT and KO with OVA for 24h and then labeled the cells with a FITC-conjugated antibody anti-CD11c. As shown in fig. 13B neither the treatment with OVA restored CD11c basal levels.

To assess whether the cell surface reduction of CD11c depends on a defect in gene expression, we analyzed the mRNA levels upon OVA treatment at the indicated times. Curiously, RT-PCR analysis revealed a significantly higher basal expression in STING KO and an induced trend upon OVA treatment (Fig. 13C).

Taken together these data suggest that STING KO macrophages attempt to compensate the absence of CD11c on the cell surface by promoting an induction of its mRNA expression.

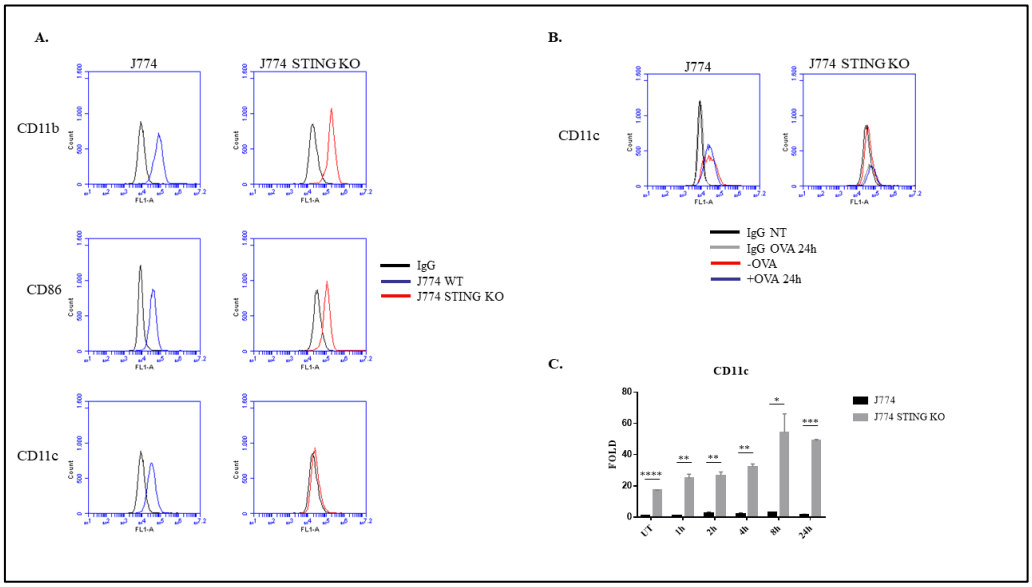

Fig 13. CD11c localization on cell surface was dampened in STING KO.

A. FACS analysis of CD11b, CD86 and CD11c at steady state. CD11c was not rescued upon 24h of OVA treatment (B). RT-PCR analysis revealed a higher CD11c expression in STING KO with an OVA-dependent induction (C). Data are representative of three independent experiment and statistical significance was evaluated by Student *t* test (* = $p<0.05$, ** = $p<0.01$, *** = $p<0.001$, **** = $p<0.0001$).

4.9 IFN-γ treatment did not induce STAT1 phosphorylation in STING KO murine cells

The cause of the absent STAT1 activation upon OVA and LPS stimuli could rely upon different mechanisms. Absent phosphorylation in STING KO could be dependent on an impaired cytokines production which act in autocrine or paracrine manner. Nevertheless, the lack of expression of stimuli-sensitive receptors on plasma membrane due to a trafficking impairment could counteract

the initiation of the signaling. In order to assess the functionality of responsiveness to a direct induction of STAT1 signaling, we treated J774 macrophages (Fig. 14A) and CT26 (Fig. 14B) with interferon gamma known to induce STAT1 phosphorylation via interferon gamma receptor (IFNGR). Surprisingly, neither J774 or CT26 responded to this stimulation when lacking STING whereas WT cells correctly respond with induction of STAT1 phosphorylation. These data suggest a possible defect in the trafficking to the plasma membrane of receptors responding to stimuli via the induction of STAT1 signaling.

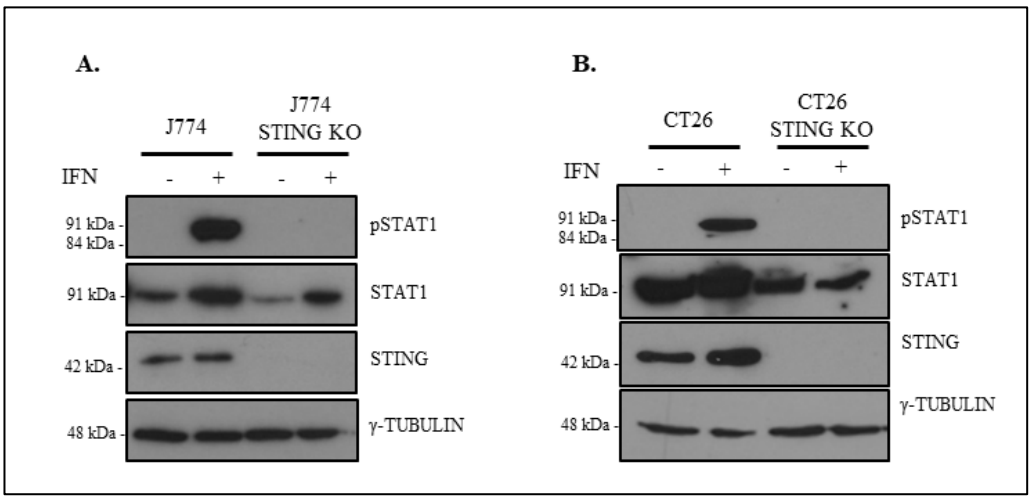

Fig 14. STAT1 was not phosphorylated upon IFN-γ treatment in STING KO cells.

J774 (A) and CT26 (B) were treated with IFN-γ for 30 minutes and the response to the stimulus was evaluated with western blot analysis. Both J774 and CT26 displayed a strong induction of STAT1 phosphorylation in WT cells whereas no activation was detected in absence of STING.

4.10 OVA-induced activation of Nf-κB is impaired in STING KO macrophages

Despite the evidences of a dampened plasma membrane receptors expression in STING KO cells, we could not exclude a defect in cytokine production. It is well known that STING induces Nf-κB signaling particularly upon LPS stimulation. To assess the role of STING in triggering OVA-dependent NF-κB activation we treated J774 cells with OVA for 1h and analyzed the nuclear translocation of its subunits. OVA-treated WT cells displayed activation of NF-κB as enlightened by nuclear translocation of p65, RelB and c-rel and degradation of IκB-α. On the other hand, STING KO macrophages revealed no activation of NF-κB (Fig. 15A). The differential responses to OVA were evaluated with an array analysis of NF-κB downstream targets. Mirroring the pattern observed in the western blot analysis, gene expression of Nf-κB subunits (c-rel, RelA and Nfkb2) and their positive regulators (Eif2ak2, Ltbr, Map3k1 and TBK1) resulted upregulated (Fig. 15B). Moreover, the basal levels of c-rel, RelA, Map3k1, Ltbr and Eif2ak2 were higher in STING KO cells then WT suggesting a compensatory mechanism attempting to restore the phenotype. TNF-α and TRAIL resulted strongly upregulated in OVA-dependent manner in WT but not in KO where TRAIL mRNA was not detected. The gene expression of Tnfaip3, a protein produced to terminate both Nf-κb and TNF-α signaling was increased in OVA-treated WT cells whereas no induction was observed in KO mirroring the different kinetics of NF-κB and TNF-α. Finally, the knock-out of STING strongly affected the transcriptional levels of membrane receptors as TLRs (2, 4 and 6) and Egfr (Fig. 15B).

Taken together these data suggest that the absence of STAT1 phosphorylation upon OVA treatment could be dependent both by a defect in receptors expression on plasma membrane and a hindered cytokine production.

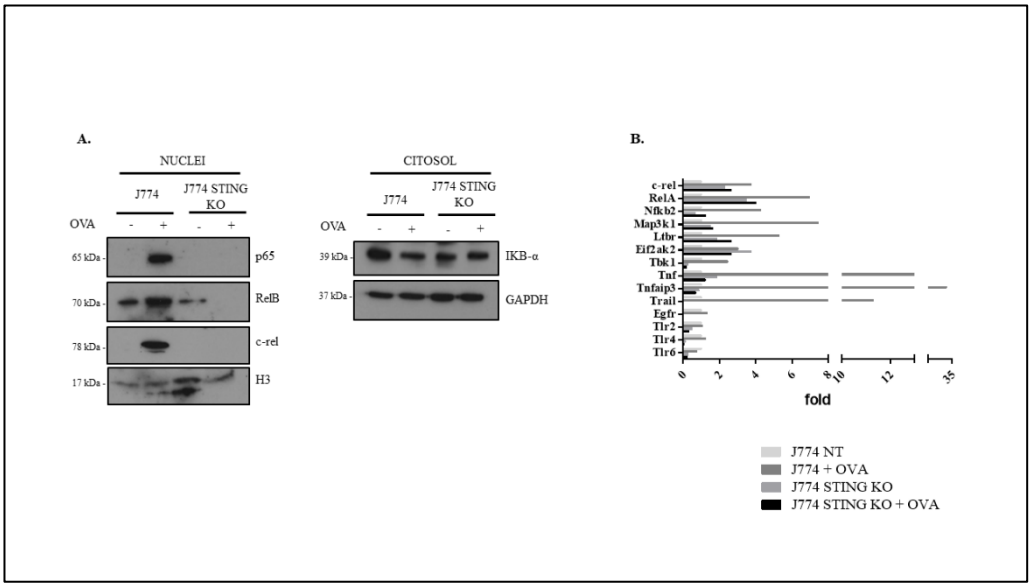

Fig. 15 Nf-κB activation was impaired in OVA-treated J774 STING KO.

J774 WT and STING KO were treated with OVA for 1h and nuclear/cytosol fractionations were performed. Western blot analysis (A) displayed a strong translocation into the nucleus of p65, RelB and c-rel in WT cells but not in STING KO. Microarray analysis (B) confirm the lack of activation of Nf-κB downstream genes in STING KO macrophages.

5. Discussion

Since its discovery in 2008 by Ishikawa et al., the role of STING in the immunity has been widely investigated. At first it was supposed to be related only to viral DNA response. Later it was shown that it is also involved in the RNA mediated response by directly interacting with RIG-I and MAVS (Nazmi 2012). From that on, it was very broadly investigated and several studies have demonstrated its role in other cellular responses beside the canonical one. The phylogenetic analysis has displayed that it is widely expressed among different species. In some cases, especially in invertebrates, it seems to be unable to activate the canonical TBK1-IRF3 response because of the lacking of the CTT domain which hinder the activation of the interferon responses (Qiu 2018). Studies on these species, have revealed that the ancient role of STING could have been different from the canonical pathway. These findings have encouraged the researchers to investigate its role in other biological processes apart from the response to nucleic acids. It was demonstrated that STING plays a central role in the autophagy regulation during innate immune response by directly interacting with LC3 so triggering the formation of autophagosomes (Liu 2019). Moreover, right after its discovery, it was found that STING interacts with MHC-II to mediate the transduction of apoptotic signals by inducing ERK activation (Jin 2008).

Even considering the canonical role in response to dsDNA the activation of STING may occur in response to a very broad range of stimuli. The initial assumption that it was triggered only by exogenous viral infection has been questioned by the demonstration that even self-DNA is able to activate it. The self-DNA can be derived either from mitochondrial leakage during pathogens infections (Zhang 2013), or by tumoral cells in an attempt to activate the immune response to counteract the tumor growth (Corrales 2015). Despite several studies have enlightened its protective role in counteract the tumor progression either by triggering T-lymphocytes tumor specific response via IFNs signaling or by

inducing an inflammatory state upon chemotherapy and radiotherapy, its role in cancer has not been completely elucidated. Indeed, STING activation have been connected to the induction of proinflammatory state that promote tumor metastasis.

Considering the central role of STING in the regulation of immunity upon infection and the capability of trigger antitumoral effects in response to neoantigens and chemo-radiotherapy we decided to investigate on its role in the process of antigen presentation.

In order to counteract the infection by foreign pathogens, cells respond to the infection by processing exogenous hosts and exposing to the plasma membrane together with MHC molecules. Depending on the origin of the antigen, the process can occur via MHC class I or class II. Cytoplasmatic antigens, derived by host infection are processed via proteasome and transferred to ER to be loaded on MHC-I. The expression on plasma membrane of the complex generates "kill me" signal that trigger $CD8^+$ T-cells cytotoxic action against the infected cell.

Exogenous antigens, derived from the phagocytosis of infected cells generate an MHC-II dependent antigen presentation. The complex MHC-II-Ag on the membrane activate $CD4^+$ dependent humoral response. However, during the endocytic pathway, a small number of proteins can escape the vesicles and enter the cytoplasm. In this case, the antigens associate to MHC-I in a mechanism named cross presentation.

The experimental model we used was designed to detect MHC-I restricted antigen presentation. By using ovalbumin, we exploit the ability of J774 macrophages to internalize an exogenous protein so mimicking an infection from exogenous pathogen. Upon the entry, OVA is proteolyzed in order to generate the correspondent antigens to interact with MHC-I. Particularly we analyzed the production of SIINFEKL by using an antibody raised against the complex MHC-I-SIINFEKL. As displayed in fig. 6, the STING KO cell line

display a dampening in the MHC-I-SIINFEKL antigen presentation. Concomitant with our study, Barnowski et al (2020) assessed a role of STING in the antigen presentation. Bone marrow dendritic cells (BMDC) derived by both WT and KO mice were incubated with feeder cells infected with an OVA-MVA. They found that BMDC derived from STING KO failed to present the MHC-I-SIINFEKL complex on the plasma membrane (Barnowski 2020).

Once confirmed its implication in the process, we investigate on the step involved in the dampening of the antigen presentation STING-dependent. First, we focused on a possible effect in the uptake of exogenous material. To assess this, we use a modified fluorescent ovalbumin conjugated with Alexa Fluor 488 to monitor the uptake from the cells. As shown in fig. 7A we find no differences between WT and STING KO cells.

Next, we investigate on the ability of the cells in correctly proteolyze the protein to generate the antigen. In order to assess this, we use DQ-OVA, a modified ovalbumin that trigger FITC fluorescence after the proteolytic cleavage. Even in this case we observe the same pattern in the WT and KO cells (Fig. 7B). Moreover, DQ-OVA fluorescence switch to red light when accumulating in the endosomal vesicles. The absence of difference between WT and KO either in the DQ-OVA generated red light suggest that, whether the defect in antigen presentation affect also MHC-II, it does not rely upon a dampening of the proteolytic process.

Next, we evaluate the correct loading of the antigen on MHC-I. Immunofluorescence analysis by using PE conjugated MHC-I-SIINFEKL revealed the presence of dots corresponding to the complex in WT cells whereas no signal was found in STING KO (Fig. 8). We then hypothesized that the limiting step occur in the peptide loading on MHC class I. During MHC-I presentation the loading of the antigen requires the action of the peptide loading complex (PLC). PLC is a transient multi-subunit ER membrane complex that orchestrate both the peptide translocation in the ER and the loading on MHC-I.

We evaluated whether the absence of the MHC-I-SIINFEKL complex could be related to these proteins. Particularly we focused on TAP1 and TAP2, the transporters that mediates the entry of antigens in the ER, and TAPBP which function as a chaperon that retain MHC-I for the correct assembly with the antigen. By analyzing the expression levels of these proteins, we found that the gene expression of TAP1, TAP2 and TAPBP were impaired in STING KO compared to WT cells. Moreover, we observed that OVA treatment induces an increase in gene expression with maximum peak at 4h. In J774 STING KO, however, OVA treatment fails to induce the same trend (Fig. 9A). Nevertheless, the analysis of protein expression does not mirror the trend seen in mRNA. WT and KO display no differences in TAP1, TAP2 and TAPBP protein levels (Fig. 9B and C). Moreover, the transcriptional increase upon 4h of OVA treatment does not result in an increase of protein expression. (Fig. 9B and C). These data suggest that even though the basal level of RNA is impaired, it is sufficient to maintain a constitutive protein production. We further investigate on a possible direct interaction of STING with PLC. We performed a Co-IP assay on J774 treated with OVA at the indicated times. SDS-PAGE display that there is no interaction between STING and TAP1 neither at basal level or upon OVA treatment (Fig. 9D).

Next, we evaluate the expression level of MHC-I. We found that in STING KO cells the presence of MHC-I in membrane is strongly reduced. Neither OVA treatment is able to rescue the basal levels found in the WT cells (Fig. 10A, B and C). We assessed whether the reason of the loss of MHC-I on plasma membrane could be dependent upon defect in mRNA. We analyzed by RT-PCR the expression levels of H2K1, the antigen presentation assay specific heavy chain, and the light chain β2m. Thel levels of H2K1 are comparable between WT and KO and there is no induction upon OVA treatment. (Fig. 10D). Otherwise, the gene expression of the light chain displays significative differences. Basal levels of β2m result lower in J774 STING KO. Besides OVA treatment slightly induces β2m expression at 4h (Fig. 10E).

β2-microglobulin is necessary for the association of MHC-I heavy chain with the PLC and for the loading of the antigen (Shields 1998). In absence of β2m, MHC-I heavy chains are not able to relocate to plasma membrane (Tatake 1992).

Drew et al. (1995) demonstrated that MHC-I gene expression regulation is triggered by Nf-κB and IRF1. IRF1 expression relies upon IFN-γ mediated induction of Jak/STAT signaling (Drew 1995). Beside the direct action on MHC-I, the IFN-γ triggering of JAK/STAT signaling also result in the induction of TAP1, TAP2 and TAPBP (Ma 1997, Seliger 2001). Because of its central role in inducing the antigen presentation, we evaluate STAT1 activation upon OVA treatment. Cells were treated with OVA at different time and activation of STAT1 was evaluated. Data shown in fig. 11 display that, upon OVA treatment STAT1 result phosphorylated on Y701. The maximum level of phosphorylation is accomplished at 4h of treatment. When STING is lacking, however, no levels of phosphorylation are detected (Fig. 11A). Intriguingly, we also observed that STING KO cells display a defect in STAT1 protein expression. By RT-PCR gene expression analysis we established that the defect in protein depends on a dampened mRNA expression (Fig 11B). The STAT1 positive feedback regulation described by Yuasa et al. (2016) may explain the increase of mRNA expression upon 4h OVA treatment which manifests with the increase of total protein observed after 8h of OVA treatment.

To further investigate the role of STING in dampening STAT1 activation we evaluate whether the response to other stimuli is still impaired. To this purpose we perform LPS treatments as showed in fig. 12A. The data reveal the same crippled pattern observed upon OVA stimulation. Moreover, the connection between STING and STAT1 is not restricted to immune cells and can be translated to human cellular systems. The same pattern of inability of triggering STAT1 activation was also found in CT26, U937 and THP-1, although the human cell lines display a residual phosphorylation indicating that

other mechanisms beside STING are involved in LPS-dependent triggering of STAT1 (Fig. 12B, C and D). However, in the human cell line we did not observe the reduction of STAT1 protein in STING KO. The link between STING and STAT signaling may be represented by PLSCR1. PLSCR1 was described to function as a Ca^{+} dependent scramblase, however it has been demonstrated to be able to translocate into the nucleus and induce the gene expression. Huang et al. (2020) demonstrated that nuclear translocation of PLSCR1 activates STAT1 expression. In addition, Karthik et al (2015) demonstrated that induction of PLSCR1 relies on STING-dependent IRF3 activation.

In order to evaluate if the lack of MHC-I on plasma membrane could be related to a trafficking impairment we analyzed the expression of other receptors. We focused on hallmark receptors of macrophages as CD11b, CD11c and CD86. We observe comparable expression of CD11b and CD86 in WT and KO whereas a very impressive decrease of CD11c was found in STING KO cell line with no rescue after OVA treatment (Fig. 13A and B). Surprisingly, the analysis of gene expression displays a very higher expression of CD11c in J774 STING KO (Fig. 13C). The positive trend observed in an OVA-dependent manner could represent a compensative mechanism that is triggered in absence of STING.

The altered expression in membrane of both MHCI and CD11c in STING KO cells could represent an evidence to explain the dampening of STAT1 signaling. Treatment with IFN-γ strongly induced STAT1 phosphorylation in WT cells whereas no induction was observed in STING KO (Fig. 14A and B). The lack of stimulation from a direct activator of STAT1 together with the altered expression of other receptors demonstrated a possible defective trafficking of proteins to plasma membrane. However, OVA and LPS treatment do not directly activate STAT1 signaling suggesting that other mechanisms, aside from trafficking defects, may participate to the altered phenotype. STING-dependent activation of Nf-κB has been widely described even though the mechanisms are still not fully elucidated. As expected, in J774 the treatment with

OVA triggered a strong nuclear translocation of Nf-κB subunits resulting in a strong gene expression increase of their downstream targets (Fig. 15A and B). In STING KO cells, however, Nf-κB activation was not observed suggesting a defect in cytokine production that, together with the dampened expression of plasma membrane receptors, may explain the alteration in STAT1 signaling.

The data described have enlightened a central role of STING in regulating antigen presentation. These findings may represent a turning point in the pathogenesis of diseases and therapeutic approaches. By positively or negatively targeting STING, beneficial effect could be obtained either in autoimmune disorders or in cancer immunotherapy. However, the comprehensive mechanism underlying this regulation are still unrevealed and require further investigations.

6. Conclusions

Data shown have elucidated a fundamental role of STING in the antigen presentation. Despite the precise mechanism is still obscure we hypothesized two different models that could explain the impairment of the process.

The first mechanism relies on STAT1 dependent signaling which was described as essential for the correct antigen presentation process. Since STAT1 is induced upon binding of ligands to receptors we hypothesized that the role of STING cold be in mediated the production of cytokines that in turn trigger the Jak/STATs signaling resulting in the MHC-I expression.

In the other model, STING is directly involved in membrane trafficking. This hypothesis could fit with its role in the formation of autophagosomes. The lack of MHC-I expression and CD11c on plasma membrane could be explained by this mechanism. In this model, the impairment of STAT1 could be a consequence of the lack of expression in membrane of receptors that induce the Jak/STAT signaling.

Both the models fit with the data accumulated and we do not exclude that the final effect could be a combination of both and that other mechanisms are involved.

7. List of publications

- Froechlich G, Gentile C, Infante L, Caiazza C, Pagano P, Scatigna S, Cotugno G, D'Alise AM, Lahm A, Scarselli E, Nicosia A, Mallardo M, Sasso E, Zambrano N. **Generation of a Novel Mesothelin-Targeted Oncolytic *Herpes* Virus and Implemented Strategies for Manufacturing.** Int J Mol Sci. 2021 Jan 6;22(2):477.

- Caiazzo E, Cerqua I, Riemma MA, Turiello R, Ialenti A, Schrader J, Fiume G, Caiazza C, Roviezzo F, Morello S, Cicala C. **Exacerbation of Allergic Airway Inflammation in Mice Lacking ECTO-5'-Nucleotidase (CD73).** Front Pharmacol. 2020 Nov 30;11:589343.

- Froechlich G, Caiazza C, Gentile C, D'Alise AM, De Lucia M, Langone F, Leoni G, Cotugno G, Scisciola V, Nicosia A, Scarselli E, Mallardo M, Sasso E, Zambrano N. **Integrity of the Antiviral STING-mediated DNA Sensing in Tumor Cells Is Required to Sustain the Immunotherapeutic Efficacy of *Herpes Simplex* Oncolytic Virus.** Cancers (Basel). 2020 Nov 17;12(11):3407.

- Caiazza C, D'Agostino M, Passaro F, Faicchia D, Mallardo M, Paladino S, Pierantoni GM, Tramontano D. **Effects of Long-Term Citrate Treatment in the PC3 Prostate Cancer Cell Line.** Int J Mol Sci. 2019 May 28;20(11):2613

- Pontoriero M, Fiume G, Vecchio E, de Laurentiis A, Albano F, Iaccino E, Mimmi S, Pisano A, Agosti V, Giovannone E, Altobelli A, Caiazza C, Mallardo M, Scala G, Quinto I. **Activation of NF-κB in B cell receptor signaling through Bruton's tyrosine kinase-dependent phosphorylation of IκB-α.** J Mol Med (Berl). 2019 May;97(5):675-690.

- Albano F, Vecchio E, Renna M, Iaccino E, Mimmi S, Caiazza C, Arcucci A, Avagliano A, Pagliara V, Donato G, Palmieri C, Mallardo M, Quinto I, Fiume G. **Insights into Thymus Development and Viral Thymic Infections.** Viruses. 2019 Sep 9;11(9):836.

- Caiazza C, Mallardo M. **The Roles of miR-25 and its Targeted Genes in Development of Human Cancer.** Microrna. 2016;5(2):113-119.

8. References

Abe T, Barber GN. Cytosolic-DNA-mediated, STING-dependent proinflammatory gene induction necessitates canonical NF-κB activation through TBK1. J Virol. 2014 May;88(10):5328-41.

Ablasser A, Goldeck M, Cavlar T, Deimling T, Witte G, Röhl I, Hopfner KP, Ludwig J, Hornung V. cGAS produces a 2'-5'-linked cyclic dinucleotide second messenger that activates STING. Nature. 2013 Jun 20;498(7454):380-4.

Adams EJ, Luoma AM. The adaptable major histocompatibility complex (MHC) fold: structure and function of nonclassical and MHC class I-like molecules. Annu Rev Immunol. 2013;31:529-61.

Ahn J, Gutman D, Saijo S, Barber GN. STING manifests self DNA-dependent inflammatory disease. Proc Natl Acad Sci U S A. 2012 Nov 20;109(47):19386-91.

Bakhoum SF, Ngo B, Laughney AM, Cavallo JA, Murphy CJ, Ly P, Shah P, Sriram RK, Watkins TBK, Taunk NK, Duran M, Pauli C, Shaw C, Chadalavada K, Rajasekhar VK, Genovese G, Venkatesan S, Birkbak NJ, McGranahan N, Lundquist M, LaPlant Q, Healey JH, Elemento O, Chung CH, Lee NY, Imielenski M, Nanjangud G, Pe'er D, Cleveland DW, Powell SN, Lammerding J, Swanton C, Cantley LC. Chromosomal instability drives metastasis through a cytosolic DNA response. Nature. 2018 Jan 25;553(7689):467-472.

Blum JS, Wearsch PA, Cresswell P. Pathways of antigen processing. Annu Rev Immunol. 2013;31:443-73.

Bouis D, Kirstetter P, Arbogast F, Lamon D, Delgado V, Jung S, Ebel C, Jacobs H, Knapp AM, Jeremiah N, Belot A, Martin T, Crow YJ, André-Schmutz I, Korganow AS, Rieux-Laucat F, Soulas-Sprauel P. Severe combined

immunodeficiency in stimulator of interferon genes (STING) V154M/wild-type mice. J Allergy Clin Immunol. 2019 Feb;143(2):712-725.e5.

Brault M, Olsen TM, Martinez J, Stetson DB, Oberst A. Intracellular Nucleic Acid Sensing Triggers Necroptosis through Synergistic Type I IFN and TNF Signaling. J Immunol. 2018 Apr 15;200(8):2748-2756.

Burdette DL, Monroe KM, Sotelo-Troha K, Iwig JS, Eckert B, Hyodo M, Hayakawa Y, Vance RE. STING is a direct innate immune sensor of cyclic di-GMP. Nature. 2011 Sep 25;478(7370):515-8.

Cao Y, Guan K, He X, Wei C, Zheng Z, Zhang Y, Ma S, Zhong H, Shi W. Yersinia YopJ negatively regulates IRF3-mediated antibacterial response through disruption of STING-mediated cytosolic DNA signaling. Biochim Biophys Acta. 2016 Dec;1863(12):3148-3159.

Cerboni S, Jeremiah N, Gentili M, Gehrmann U, Conrad C, Stolzenberg MC, Picard C, Neven B, Fischer A, Amigorena S, Rieux-Laucat F, Manel N. Intrinsic antiproliferative activity of the innate sensor STING in T lymphocytes. J Exp Med. 2017 Jun 5;214(6):1769-1785.

Chen H, Sun H, You F, Sun W, Zhou X, Chen L, Yang J, Wang Y, Tang H, Guan Y, Xia W, Gu J, Ishikawa H, Gutman D, Barber G, Qin Z, Jiang Z. Activation of STAT6 by STING is critical for antiviral innate immunity. Cell. 2011 Oct 14;147(2):436-46.

Chen M, Meng Q, Qin Y, Liang P, Tan P, He L, Zhou Y, Chen Y, Huang J, Wang RF, Cui J. TRIM14 Inhibits cGAS Degradation Mediated by Selective Autophagy Receptor p62 to Promote Innate Immune Responses. Mol Cell. 2016 Oct 6;64(1):105-119.

Chen Q, Boire A, Jin X, Valiente M, Er EE, Lopez-Soto A, Jacob L, Patwa R, Shah H, Xu K, Cross JR, Massagué J. Carcinoma-astrocyte gap junctions promote brain metastasis by cGAMP transfer. Nature. 2016 May 26;533(7604):493-498.

Chen Y, Wang L, Jin J, Luan Y, Chen C, Li Y, Chu H, Wang X, Liao G, Yu Y, Teng H, Wang Y, Pan W, Fang L, Liao L, Jiang Z, Ge X, Li B, Wang P. p38 inhibition provides anti-DNA virus immunity by regulation of USP21 phosphorylation and STING activation. J Exp Med. 2017 Apr 3;214(4):991-1010.

Chon HJ, Kim H, Noh JH, Yang H, Lee WS, Kong SJ, Lee SJ, Lee YS, Kim WR, Kim JH, Kim G, Kim C. STING signaling is a potential immunotherapeutic target in colorectal cancer. J Cancer. 2019 Aug 27;10(20):4932-4938.

Christensen MH, Jensen SB, Miettinen JJ, Luecke S, Prabakaran T, Reinert LS, Mettenleiter T, Chen ZJ, Knipe DM, Sandri-Goldin RM, Enquist LW, Hartmann R, Mogensen TH, Rice SA, Nyman TA, Matikainen S, Paludan SR. HSV-1 ICP27 targets the TBK1-activated STING signalsome to inhibit virus-induced type I IFN expression. EMBO J. 2016 Jul 1;35(13):1385-99.

Corrales L, Glickman LH, McWhirter SM, Kanne DB, Sivick KE, Katibah GE, Woo SR, Lemmens E, Banda T, Leong JJ, Metchette K, Dubensky TW Jr, Gajewski TF. Direct Activation of STING in the Tumor Microenvironment Leads to Potent and Systemic Tumor Regression and Immunity. Cell Rep. 2015 May 19;11(7):1018-30.

Crow YJ, Hayward BE, Parmar R, Robins P, Leitch A, Ali M, Black DN, van Bokhoven H, Brunner HG, Hamel BC, Corry PC, Cowan FM, Frints SG, Klepper J, Livingston JH, Lynch SA, Massey RF, Meritet JF, Michaud JL, Ponsot G, Voit T, Lebon P, Bonthron DT, Jackson AP, Barnes DE, Lindahl T. Mutations in the gene encoding the 3'-5' DNA exonuclease TREX1 cause Aicardi-Goutières syndrome at the AGS1 locus. Nat Genet. 2006 Aug;38(8):917-20.

Cui Y, Zhao D, Sreevatsan S, Liu C, Yang W, Song Z, Yang L, Barrow P, Zhou X. *Mycobacterium bovis* Induces Endoplasmic Reticulum Stress Mediated-

Apoptosis by Activating IRF3 in a Murine Macrophage Cell Line. Front Cell Infect Microbiol. 2016 Dec 12;6:182.

Dai J, Huang YJ, He X, Zhao M, Wang X, Liu ZS, Xue W, Cai H, Zhan XY, Huang SY, He K, Wang H, Wang N, Sang Z, Li T, Han QY, Mao J, Diao X, Song N, Chen Y, Li WH, Man JH, Li AL, Zhou T, Liu ZG, Zhang XM, Li T. Acetylation Blocks cGAS Activity and Inhibits Self-DNA-Induced Autoimmunity. Cell. 2019 Mar 7;176(6):1447-1460.e14.

Demaria O, De Gassart A, Coso S, Gestermann N, Di Domizio J, Flatz L, Gaide O, Michielin O, Hwu P, Petrova TV, Martinon F, Modlin RL, Speiser DE, Gilliet M. STING activation of tumor endothelial cells initiates spontaneous and therapeutic antitumor immunity. Proc Natl Acad Sci U S A. 2015 Dec 15;112(50):15408-13.

Deschamps T, Kalamvoki M. Evasion of the STING DNA-Sensing Pathway by VP11/12 of Herpes Simplex Virus 1. J Virol. 2017 Jul 27;91(16):e00535-17.

Dey RJ, Dey B, Zheng Y, Cheung LS, Zhou J, Sayre D, Kumar P, Guo H, Lamichhane G, Sintim HO, Bishai WR. Inhibition of innate immune cytosolic surveillance by an M. tuberculosis phosphodiesterase. Nat Chem Biol. 2017 Feb;13(2):210-217.

Dobbs N, Burnaevskiy N, Chen D, Gonugunta VK, Alto NM, Yan N. STING Activation by Translocation from the ER Is Associated with Infection and Autoinflammatory Disease. Cell Host Microbe. 2015 Aug 12;18(2):157-68.

Drew PD, Franzoso G, Becker KG, Bours V, Carlson LM, Siebenlist U, Ozato K. NF kappa B and interferon regulatory factor 1 physically interact and synergistically induce major histocompatibility class I gene expression. J Interferon Cytokine Res. 1995 Dec;15(12):1037-45.

Du M, Chen ZJ. DNA-induced liquid phase condensation of cGAS activates innate immune signaling. Science. 2018 Aug 17;361(6403):704-709.

Eaglesham JB, Pan Y, Kupper TS, Kranzusch PJ. Viral and metazoan poxins are cGAMP-specific nucleases that restrict cGAS-STING signalling. Nature. 2019 Feb;566(7743):259-263.

Fang R, Wang C, Jiang Q, Lv M, Gao P, Yu X, Mu P, Zhang R, Bi S, Feng JM, Jiang Z. NEMO-IKKβ Are Essential for IRF3 and NF-κB Activation in the cGAS-STING Pathway. J Immunol. 2017 Nov 1;199(9):3222-3233.

Ferguson BJ, Mansur DS, Peters NE, Ren H, Smith GL. DNA-PK is a DNA sensor for IRF-3-dependent innate immunity. Elife. 2012 Dec 18;1:e00047.

Fu J, Kanne DB, Leong M, Glickman LH, McWhirter SM, Lemmens E, Mechette K, Leong JJ, Lauer P, Liu W, Sivick KE, Zeng Q, Soares KC, Zheng L, Portnoy DA, Woodward JJ, Pardoll DM, Dubensky TW Jr, Kim Y. STING agonist formulated cancer vaccines can cure established tumors resistant to PD-1 blockade. Sci Transl Med. 2015 Apr 15;7(283):283ra52.

Fu YZ, Guo Y, Zou HM, Su S, Wang SY, Yang Q, Luo MH, Wang YY. Human cytomegalovirus protein UL42 antagonizes cGAS/MITA-mediated innate antiviral response. PLoS Pathog. 2019 May 20;15(5):e1007691.

Fu YZ, Su S, Gao YQ, Wang PP, Huang ZF, Hu MM, Luo WW, Li S, Luo MH, Wang YY, Shu HB. Human Cytomegalovirus Tegument Protein UL82 Inhibits STING-Mediated Signaling to Evade Antiviral Immunity. Cell Host Microbe. 2017 Feb 8;21(2):231-243.

Gaidt MM, Ebert TS, Chauhan D, Ramshorn K, Pinci F, Zuber S, O'Duill F, Schmid-Burgk JL, Hoss F, Buhmann R, Wittmann G, Latz E, Subklewe M, Hornung V. The DNA Inflammasome in Human Myeloid Cells Is Initiated by a STING-Cell Death Program Upstream of NLRP3. Cell. 2017 Nov 16;171(5):1110-1124.e18.

Gamage AM, Lee KO, Gan YH. Anti-Cancer Drug HMBA Acts as an Adjuvant during Intracellular Bacterial Infections by Inducing Type I IFN through STING. J Immunol. 2017 Oct 1;199(7):2491-2502.

Gao D, Li T, Li XD, Chen X, Li QZ, Wight-Carter M, Chen ZJ. Activation of cyclic GMP-AMP synthase by self-DNA causes autoimmune diseases. Proc Natl Acad Sci U S A. 2015 Oct 20;112(42):E5699-705.

Gao M, He Y, Tang H, Chen X, Liu S, Tao Y. cGAS/STING: novel perspectives of the classic pathway. Mol Biomed. 2020. Sep 20; 1, 7.

Gaston J, Cheradame L, Yvonnet V, Deas O, Poupon MF, Judde JG, Cairo S, Goffin V. Intracellular STING inactivation sensitizes breast cancer cells to genotoxic agents. Oncotarget. 2016 Nov 22;7(47):77205-77224.

Geijtenbeek TB, Gringhuis SI. Signalling through C-type lectin receptors: shaping immune responses. Nat Rev Immunol. 2009 Jul;9(7):465-79.

Glück S, Guey B, Gulen MF, Wolter K, Kang TW, Schmacke NA, Bridgeman A, Rehwinkel J, Zender L, Ablasser A. Innate immune sensing of cytosolic chromatin fragments through cGAS promotes senescence. Nat Cell Biol. 2017 Sep;19(9):1061-1070.

Goto A, Okado K, Martins N, Cai H, Barbier V, Lamiable O, Troxler L, Santiago E, Kuhn L, Paik D, Silverman N, Holleufer A, Hartmann R, Liu J, Peng T, Hoffmann JA, Meignin C, Daeffler L, Imler JL. The Kinase IKKβ Regulates a STING- and NF-κB-Dependent Antiviral Response Pathway in Drosophila. Immunity. 2018 Aug 21;49(2):225-234.e4.

Gui X, Yang H, Li T, Tan X, Shi P, Li M, Du F, Chen ZJ. Autophagy induction via STING trafficking is a primordial function of the cGAS pathway. Nature. 2019 Mar;567(7747):262-266.

Guimarães ES, Gomes MTR, Campos PC, Mansur DS, Dos Santos AA, Harms J, Splitter G, Smith JA, Barber GN, Oliveira SC. *Brucella abortus* Cyclic Dinucleotides Trigger STING-Dependent Unfolded Protein Response That Favors Bacterial Replication. J Immunol. 2019 May 1;202(9):2671-2681.

Haag SM, Gulen MF, Reymond L, Gibelin A, Abrami L, Decout A, Heymann M, van der Goot FG, Turcatti G, Behrendt R, Ablasser A. Targeting STING with covalent small-molecule inhibitors. Nature. 2018 Jul;559(7713):269-273.

Hansen AL, Buchan GJ, Rühl M, Mukai K, Salvatore SR, Ogawa E, Andersen SD, Iversen MB, Thielke AL, Gunderstofte C, Motwani M, Møller CT, Jakobsen AS, Fitzgerald KA, Roos J, Lin R, Maier TJ, Goldbach-Mansky R, Miner CA, Qian W, Miner JJ, Rigby RE, Rehwinkel J, Jakobsen MR, Arai H, Taguchi T, Schopfer FJ, Olagnier D, Holm CK. Nitro-fatty acids are formed in response to virus infection and are potent inhibitors of STING palmitoylation and signaling. Proc Natl Acad Sci U S A. 2018 Aug 14;115(33):E7768-E7775.

Harrington KJ, Brody J, Ingham M, Strauss J, Cemerski S, Wang M, Tse A, Khilnani A, Marabelle A, Golan T. Preliminary results of the first-in-human (FIH) study of MK-1454, an agonist of stimulator of interferon genes (STING), as monotherapy or in combination with pembrolizumab (pembro) in patients with advanced solid tumors or lymphomas. Ann. Oncol. 2018 29, 712-712

Härtlova A, Erttmann SF, Raffi FA, Schmalz AM, Resch U, Anugula S, Lienenklaus S, Nilsson LM, Kröger A, Nilsson JA, Ek T, Weiss S, Gekara NO. DNA damage primes the type I interferon system via the cytosolic DNA sensor STING to promote anti-microbial innate immunity. Immunity. 2015 Feb 17;42(2):332-343.

Haughey CM, Mukherjee D, Steele RE, Popple A, Dura-Perez L, Pickard A, Patel M, Jain S, Mullan PB, Williams R, Oliveira P, Buckley NE, Honeychurch J, S McDade S, Illidge T, Mills IG, Eddie SL. Investigating Radiotherapy Response in a Novel Syngeneic Model of Prostate Cancer. Cancers (Basel). 2020 Sep 29;12(10):2804.

Hebert DN, Garman SC, Molinari M. The glycan code of the endoplasmic reticulum: asparagine-linked carbohydrates as protein maturation and quality-control tags. Trends Cell Biol. 2005 Jul;15(7):364-70.

Holm CK, Jensen SB, Jakobsen MR, Cheshenko N, Horan KA, Moeller HB, Gonzalez-Dosal R, Rasmussen SB, Christensen MH, Yarovinsky TO, Rixon FJ, Herold BC, Fitzgerald KA, Paludan SR. Virus-cell fusion as a trigger of innate immunity dependent on the adaptor STING. Nat Immunol. 2012 Jun 17;13(8):737-43.

Hu MM, Yang Q, Xie XQ, Liao CY, Lin H, Liu TT, Yin L, Shu HB. Sumoylation Promotes the Stability of the DNA Sensor cGAS and the Adaptor STING to Regulate the Kinetics of Response to DNA Virus. Immunity. 2016 Sep 20;45(3):555-569.

Huang J, You H, Su C, Li Y, Chen S, Zheng C. Herpes Simplex Virus 1 Tegument Protein VP22 Abrogates cGAS/STING-Mediated Antiviral Innate Immunity. J Virol. 2018 Jul 17;92(15):e00841-18.

Huang P, Liao R, Chen X, Wu X, Li X, Wang Y, Cao Q, Dong C. Nuclear translocation of PLSCR1 activates STAT1 signaling in basal-like breast cancer. Theranostics. 2020 Mar 25;10(10):4644-4658.

Huang YH, Liu XY, Du XX, Jiang ZF, Su XD. The structural basis for the sensing and binding of cyclic di-GMP by STING. Nat Struct Mol Biol. 2012 Jun 24;19(7):728-30.

Ishikawa H, Barber GN. STING is an endoplasmic reticulum adaptor that facilitates innate immune signalling. Nature. 2008 Oct 2;455(7213):674-8.

Jin L, Waterman PM, Jonscher KR, Short CM, Reisdorph NA, Cambier JC. MPYS, a novel membrane tetraspanner, is associated with major histocompatibility complex class II and mediates transduction of apoptotic signals. Mol Cell Biol. 2008 Aug;28(16):5014-26.

Jin L, Xu LG, Yang IV, Davidson EJ, Schwartz DA, Wurfel MM, Cambier JC. Identification and characterization of a loss-of-function human MPYS variant. Genes Immun. 2011 Jun;12(4):263-9.

Kalamvoki M, Roizman B. HSV-1 degrades, stabilizes, requires, or is stung by STING depending on ICP0, the US3 protein kinase, and cell derivation. Proc Natl Acad Sci U S A. 2014 Feb 4;111(5):E611-7.

Kato K, Ishii R, Goto E, Ishitani R, Tokunaga F, Nureki O. Structural and functional analyses of DNA-sensing and immune activation by human cGAS. PLoS One. 2013 Oct 7;8(10):e76983.

Kawane K, Fukuyama H, Kondoh G, Takeda J, Ohsawa Y, Uchiyama Y, Nagata S. Requirement of DNase II for definitive erythropoiesis in the mouse fetal liver. Science. 2001 May 25;292(5521):1546-9.

Kawane K, Ohtani M, Miwa K, Kizawa T, Kanbara Y, Yoshioka Y, Yoshikawa H, Nagata S. Chronic polyarthritis caused by mammalian DNA that escapes from degradation in macrophages. Nature. 2006 Oct 26;443(7114):998-1002.

Kelley N, Jeltema D, Duan Y, He Y. The NLRP3 Inflammasome: An Overview of Mechanisms of Activation and Regulation. Int J Mol Sci. 2019 Jul 6;20(13):3328.

Kim JE, Kim YE, Stinski MF, Ahn JH, Song YJ. Human Cytomegalovirus IE2 86 kDa Protein Induces STING Degradation and Inhibits cGAMP-Mediated IFN-β Induction. Front Microbiol. 2017 Sep 26;8:1854.

Kitai Y, Kawasaki T, Sueyoshi T, Kobiyama K, Ishii KJ, Zou J, Akira S, Matsuda T, Kawai T. DNA-Containing Exosomes Derived from Cancer Cells Treated with Topotecan Activate a STING-Dependent Pathway and Reinforce Antitumor Immunity. J Immunol. 2017 Feb 15;198(4):1649-1659.

Kodigepalli KM, Nanjundan M. Induction of PLSCR1 in a STING/IRF3-dependent manner upon vector transfection in ovarian epithelial cells. PLoS One. 2015 Feb 6;10(2):e0117464.

Konno H, Konno K, Barber GN. Cyclic dinucleotides trigger ULK1 (ATG1) phosphorylation of STING to prevent sustained innate immune signaling. Cell. 2013 Oct 24;155(3):688-98.

Kwon D, Sesaki H, Kang SJ. Intracellular calcium is a rheostat for the STING signaling pathway. Biochem Biophys Res Commun. 2018 Jun 2;500(2):497-503.

Lan YY, Heather JM, Eisenhaure T, Garris CS, Lieb D, Raychowdhury R, Hacohen N. Extranuclear DNA accumulates in aged cells and contributes to senescence and inflammation. Aging Cell. 2019 Apr;18(2):e12901.

Landsverk OJ, Bakke O, Gregers TF. MHC II and the endocytic pathway: regulation by invariant chain. Scand J Immunol. 2009 Sep;70(3):184-93.

Lee MN, Roy M, Ong SE, Mertins P, Villani AC, Li W, Dotiwala F, Sen J, Doench JG, Orzalli MH, Kramnik I, Knipe DM, Lieberman J, Carr SA, Hacohen N. Identification of regulators of the innate immune response to cytosolic DNA and retroviral infection by an integrative approach. Nat Immunol. 2013 Feb;14(2):179-85.

Lemaitre B, Nicolas E, Michaut L, Reichhart JM, Hoffmann JA. The dorsoventral regulatory gene cassette spätzle/Toll/cactus controls the potent antifungal response in Drosophila adults. Cell. 1996 Sep 20;86(6):973-83.

Lemos H, Huang L, Chandler PR, Mohamed E, Souza GR, Li L, Pacholczyk G, Barber GN, Hayakawa Y, Munn DH, Mellor AL. Activation of the STING adaptor attenuates experimental autoimmune encephalitis. J Immunol. 2014 Jun 15;192(12):5571-8.

Li X, Shu C, Yi G, Chaton CT, Shelton CL, Diao J, Zuo X, Kao CC, Herr AB, Li P. Cyclic GMP-AMP synthase is activated by double-stranded DNA-induced oligomerization. Immunity. 2013 Dec 12;39(6):1019-31.

Li Z, Liu G, Sun L, Teng Y, Guo X, Jia J, Sha J, Yang X, Chen D, Sun Q. PPM1A regulates antiviral signaling by antagonizing TBK1-mediated STING phosphorylation and aggregation. PLoS Pathog. 2015 Mar 27;11(3):e1004783.

Liang D, Xiao-Feng H, Guan-Jun D, Er-Ling H, Sheng C, Ting-Ting W, Qin-Gang H, Yan-Hong N, Ya-Yi H. Activated STING enhances Tregs infiltration in the HPV-related carcinogenesis of tongue squamous cells via the c-jun/CCL22 signal. Biochim Biophys Acta. 2015 Nov;1852(11):2494-503.

Liu D, Wu H, Wang C, Li Y, Tian H, Siraj S, Sehgal SA, Wang X, Wang J, Shang Y, Jiang Z, Liu L, Chen Q. STING directly activates autophagy to tune the innate immune response. Cell Death Differ. 2019 Sep;26(9):1735-1749.

Liu H, Zhang H, Wu X, Ma D, Wu J, Wang L, Jiang Y, Fei Y, Zhu C, Tan R, Jungblut P, Pei G, Dorhoi A, Yan Q, Zhang F, Zheng R, Liu S, Liang H, Liu Z, Yang H, Chen J, Wang P, Tang T, Peng W, Hu Z, Xu Z, Huang X, Wang J, Li H, Zhou Y, Liu F, Yan D, Kaufmann SHE, Chen C, Mao Z, Ge B. Nuclear cGAS suppresses DNA repair and promotes tumorigenesis. Nature. 2018 Nov;563(7729):131-136.

Liu S, Cai X, Wu J, Cong Q, Chen X, Li T, Du F, Ren J, Wu YT, Grishin NV, Chen ZJ. Phosphorylation of innate immune adaptor proteins MAVS, STING, and TRIF induces IRF3 activation. Science. 2015 Mar 13;347(6227):aaa2630.

Liu S, Cai X, Wu J, Cong Q, Chen X, Li T, Du F, Ren J, Wu YT, Grishin NV, Chen ZJ. Phosphorylation of innate immune adaptor proteins MAVS, STING, and TRIF induces IRF3 activation. Science. 2015 Mar 13;347(6227):aaa2630.

Liu W, Reyes HM, Yang JF, Li Y, Stewart KM, Basil MC, Lin SM, Katzen J, Morrisey EE, Weiss SR, You J. Activation of STING signaling pathway effectively blocks human coronavirus infection. J Virol. 2021 Mar 31:JVI.00490-21.

Liu Y, Gordesky-Gold B, Leney-Greene M, Weinbren NL, Tudor M, Cherry S. Inflammation-Induced, STING-Dependent Autophagy Restricts Zika Virus

Infection in the Drosophila Brain. Cell Host Microbe. 2018 Jul 11;24(1):57-68.e3.

Liu Y, Jesus AA, Marrero B, Yang D, Ramsey SE, Sanchez GAM, Tenbrock K, Wittkowski H, Jones OY, Kuehn HS, Lee CR, DiMattia MA, Cowen EW, Gonzalez B, Palmer I, DiGiovanna JJ, Biancotto A, Kim H, Tsai WL, Trier AM, Huang Y, Stone DL, Hill S, Kim HJ, St Hilaire C, Gurprasad S, Plass N, Chapelle D, Horkayne-Szakaly I, Foell D, Barysenka A, Candotti F, Holland SM, Hughes JD, Mehmet H, Issekutz AC, Raffeld M, McElwee J, Fontana JR, Minniti CP, Moir S, Kastner DL, Gadina M, Steven AC, Wingfield PT, Brooks SR, Rosenzweig SD, Fleisher TA, Deng Z, Boehm M, Paller AS, Goldbach-Mansky R. Activated STING in a vascular and pulmonary syndrome. N Engl J Med. 2014 Aug 7;371(6):507-518.

Liu Y, Jesus AA, Marrero B, Yang D, Ramsey SE, Sanchez GAM, Tenbrock K, Wittkowski H, Jones OY, Kuehn HS, Lee CR, DiMattia MA, Cowen EW, Gonzalez B, Palmer I, DiGiovanna JJ, Biancotto A, Kim H, Tsai WL, Trier AM, Huang Y, Stone DL, Hill S, Kim HJ, St Hilaire C, Gurprasad S, Plass N, Chapelle D, Horkayne-Szakaly I, Foell D, Barysenka A, Candotti F, Holland SM, Hughes JD, Mehmet H, Issekutz AC, Raffeld M, McElwee J, Fontana JR, Minniti CP, Moir S, Kastner DL, Gadina M, Steven AC, Wingfield PT, Brooks SR, Rosenzweig SD, Fleisher TA, Deng Z, Boehm M, Paller AS, Goldbach-Mansky R. Activated STING in a vascular and pulmonary syndrome. N Engl J Med. 2014 Aug 7;371(6):507-518.

Livak KJ, Schmittgen TD. Analysis of relative gene expression data using real-time quantitative PCR and the 2(-Delta Delta C(T)) Method. Methods. 2001 Dec;25(4):402-8.

Luecke S, Holleufer A, Christensen MH, Jønsson KL, Boni GA, Sørensen LK, Johannsen M, Jakobsen MR, Hartmann R, Paludan SR. cGAS is activated by DNA in a length-dependent manner. EMBO Rep. 2017 Oct;18(10):1707-1715.

Luo WW, Li S, Li C, Lian H, Yang Q, Zhong B, Shu HB. iRhom2 is essential for innate immunity to DNA viruses by mediating trafficking and stability of the adaptor STING. Nat Immunol. 2016 Sep;17(9):1057-66.

Luteijn RD, Zaver SA, Gowen BG, Wyman SK, Garelis NE, Onia L, McWhirter SM, Katibah GE, Corn JE, Woodward JJ, Raulet DH. SLC19A1 transports immunoreactive cyclic dinucleotides. Nature. 2019 Sep;573(7774):434-438.

Ma W, Lehner PJ, Cresswell P, Pober JS, Johnson DR. Interferon-gamma rapidly increases peptide transporter (TAP) subunit expression and peptide transport capacity in endothelial cells. J Biol Chem. 1997 Jun 27;272(26):16585-90.

Ma Z, Jacobs SR, West JA, Stopford C, Zhang Z, Davis Z, Barber GN, Glaunsinger BA, Dittmer DP, Damania B. Modulation of the cGAS-STING DNA sensing pathway by gammaherpesviruses. Proc Natl Acad Sci U S A. 2015 Aug 4;112(31):E4306-15.

Mackenzie KJ, Carroll P, Martin CA, Murina O, Fluteau A, Simpson DJ, Olova N, Sutcliffe H, Rainger JK, Leitch A, Osborn RT, Wheeler AP, Nowotny M, Gilbert N, Chandra T, Reijns MAM, Jackson AP. cGAS surveillance of micronuclei links genome instability to innate immunity. Nature. 2017 Aug 24;548(7668):461-465.

Marcus A, Mao AJ, Lensink-Vasan M, Wang L, Vance RE, Raulet DH. Tumor-Derived cGAMP Triggers a STING-Mediated Interferon Response in Non-tumor Cells to Activate the NK Cell Response. Immunity. 2018 Oct 16;49(4):754-763.e4.

Martin M, Hiroyasu A, Guzman RM, Roberts SA, Goodman AG. Analysis of Drosophila STING Reveals an Evolutionarily Conserved Antimicrobial Function. Cell Rep. 2018 Jun 19;23(12):3537-3550.e6.

Martin TL, Jee J, Kim E, Steiner HE, Cormet-Boyaka E, Boyaka PN. Sublingual targeting of STING with 3'3'-cGAMP promotes systemic and mucosal immunity against anthrax toxins. Vaccine. 2017 Apr 25;35(18):2511-2519.

Mathur V, Burai R, Vest RT, Bonanno LN, Lehallier B, Zardeneta ME, Mistry KN, Do D, Marsh SE, Abud EM, Blurton-Jones M, Li L, Lashuel HA, Wyss-Coray T. Activation of the STING-Dependent Type I Interferon Response Reduces Microglial Reactivity and Neuroinflammation. Neuron. 2017 Dec 20;96(6):1290-1302.e6.

Meade N, Furey C, Li H, Verma R, Chai Q, Rollins MG, DiGiuseppe S, Naghavi MH, Walsh D. Poxviruses Evade Cytosolic Sensing through Disruption of an mTORC1-mTORC2 Regulatory Circuit. Cell. 2018 Aug 23;174(5):1143-1157.e17.

Melki I, Rose Y, Uggenti C, Van Eyck L, Frémond ML, Kitabayashi N, Rice GI, Jenkinson EM, Boulai A, Jeremiah N, Gattorno M, Volpi S, Sacco O, Terheggen-Lagro SWJ, Tiddens HAWM, Meyts I, Morren MA, De Haes P, Wouters C, Legius E, Corveleyn A, Rieux-Laucat F, Bodemer C, Callebaut I, Rodero MP, Crow YJ. Disease-associated mutations identify a novel region in human STING necessary for the control of type I interferon signaling. J Allergy Clin Immunol. 2017 Aug;140(2):543-552.e5.

Meric-Bernstam F, Sandhu SK, Hamid O, Spreafico A, Kasper S, Dummer R, Shimizu T, Steeghs N, Lewis N, Talluto CC, Dolan S, Bean A, Brown R, Trujillo D, Nair N, Luke JJ. Phase Ib study of MIW815 (ADU-S100) in combination with spartalizumab (PDR001) in patients (pts) with advanced/metastatic solid tumors or lymphomas. Journal of Clinical Oncology 2019 37:15_suppl, 2507-2507

Moretti J, Roy S, Bozec D, Martinez J, Chapman JR, Ueberheide B, Lamming DW, Chen ZJ, Horng T, Yeretssian G, Green DR, Blander JM. STING Senses

Microbial Viability to Orchestrate Stress-Mediated Autophagy of the Endoplasmic Reticulum. Cell. 2017 Nov 2;171(4):809-823.e13.

Morita M, Stamp G, Robins P, Dulic A, Rosewell I, Hrivnak G, Daly G, Lindahl T, Barnes DE. Gene-targeted mice lacking the Trex1 (DNase III) 3'-->5' DNA exonuclease develop inflammatory myocarditis. Mol Cell Biol. 2004 Aug;24(15):6719-27.

MPYS/STING-mediated TNF-α, not type I IFN, is essential for the mucosal adjuvant activity of (3'-5')-cyclic-di-guanosine-monophosphate in vivo. J Immunol. 2014 Jan 1;192(1):492-502.

Mukai K, Konno H, Akiba T, Uemura T, Waguri S, Kobayashi T, Barber GN, Arai H, Taguchi T. Activation of STING requires palmitoylation at the Golgi. Nat Commun. 2016 Jun 21;7:11932.

Nazmi A, Field RH, Griffin EW, Haugh O, Hennessy E, Cox D, Reis R, Tortorelli L, Murray CL, Lopez-Rodriguez AB, Jin L, Lavelle EC, Dunne A, Cunningham C. Chronic neurodegeneration induces type I interferon synthesis via STING, shaping microglial phenotype and accelerating disease progression. Glia. 2019 Jul;67(7):1254-1276.

Nazmi A, Mukhopadhyay R, Dutta K, Basu A. STING mediates neuronal innate immune response following Japanese encephalitis virus infection. Sci Rep. 2012;2:347.

Ni G, Konno H, Barber GN. Ubiquitination of STING at lysine 224 controls IRF3 activation. Sci Immunol. 2017 May 5;2(11):eaah7119.

Oancea G, O'Mara ML, Bennett WF, Tieleman DP, Abele R, Tampé R. Structural arrangement of the transmission interface in the antigen ABC transport complex TAP. Proc Natl Acad Sci U S A. 2009 Apr 7;106(14):5551-6.

Ortmann B, Copeman J, Lehner PJ, Sadasivan B, Herberg JA, Grandea AG, Riddell SR, Tampé R, Spies T, Trowsdale J, Cresswell P. A critical role for tapasin in the assembly and function of multimeric MHC class I-TAP complexes. Science. 1997 Aug 29;277(5330):1306-9.

Patel S, Blaauboer SM, Tucker HR, Mansouri S, Ruiz-Moreno JS, Hamann L, Schumann RR, Opitz B, Jin L. The Common R71H-G230A-R293Q Human TMEM173 Is a Null Allele. J Immunol. 2017 Jan 15;198(2):776-787.

Peng Y, Zhuang J, Ying G, Zeng H, Zhou H, Cao Y, Chen H, Xu C, Fu X, Xu H, Li J, Cao S, Chen J, Gu C, Yan F, Chen G. Stimulator of IFN genes mediates neuroinflammatory injury by suppressing AMPK signal in experimental subarachnoid hemorrhage. J Neuroinflammation. 2020 May 25;17(1):165.

Petrasek J, Iracheta-Vellve A, Csak T, Satishchandran A, Kodys K, Kurt-Jones EA, Fitzgerald KA, Szabo G. STING-IRF3 pathway links endoplasmic reticulum stress with hepatocyte apoptosis in early alcoholic liver disease. Proc Natl Acad Sci U S A. 2013 Oct 8;110(41):16544-9.

Prantner D, Perkins DJ, Lai W, Williams MS, Sharma S, Fitzgerald KA, Vogel SN. 5,6-Dimethylxanthenone-4-acetic acid (DMXAA) activates stimulator of interferon gene (STING)-dependent innate immune pathways and is regulated by mitochondrial membrane potential. J Biol Chem. 2012 Nov 16;287(47):39776-88.

Qin Y, Zhou MT, Hu MM, Hu YH, Zhang J, Guo L, Zhong B, Shu HB. RNF26 temporally regulates virus-triggered type I interferon induction by two distinct mechanisms. PLoS Pathog. 2014 Sep 25;10(9):e1004358.

Qiu Y, Zhou X. STING: From Mammals to Insects. Cell Host Microbe. 2018 Jul 11;24(1):5-7.

Ramanjulu JM, Pesiridis GS, Yang J, Concha N, Singhaus R, Zhang SY, Tran JL, Moore P, Lehmann S, Eberl HC, Muelbaier M, Schneck JL, Clemens J, Adam M, Mehlmann J, Romano J, Morales A, Kang J, Leister L, Graybill TL,

Charnley AK, Ye G, Nevins N, Behnia K, Wolf AI, Kasparcova V, Nurse K, Wang L, Puhl AC, Li Y, Klein M, Hopson CB, Guss J, Bantscheff M, Bergamini G, Reilly MA, Lian Y, Duffy KJ, Adams J, Foley KP, Gough PJ, Marquis RW, Smothers J, Hoos A, Bertin J. Design of amidobenzimidazole STING receptor agonists with systemic activity. Nature. 2018 Dec;564(7736):439-443.

Rasaiyaah J, Tan CP, Fletcher AJ, Price AJ, Blondeau C, Hilditch L, Jacques DA, Selwood DL, James LC, Noursadeghi M, Towers GJ. HIV-1 evades innate immune recognition through specific cofactor recruitment. Nature. 2013 Nov 21;503(7476):402-405.

Rehwinkel J, Gack MU. RIG-I-like receptors: their regulation and roles in RNA sensing. *Nat Rev Immunol*. 2020;20(9):537-551.

Rice GI, Rodero MP, Crow YJ. Human disease phenotypes associated with mutations in TREX1. J Clin Immunol. 2015 Apr;35(3):235-43.

Rui Y, Su J, Shen S, Hu Y, Huang D, Zheng W, Lou M, Shi Y, Wang M, Chen S, Zhao N, Dong Q, Cai Y, Xu R, Zheng S, Yu XF. Unique and complementary suppression of cGAS-STING and RNA sensing- triggered innate immune responses by SARS-CoV-2 proteins. Signal Transduct Target Ther. 2021 Mar 15;6(1):123.

Saveanu L, Carroll O, Lindo V, Del Val M, Lopez D, Lepelletier Y, Greer F, Schomburg L, Fruci D, Niedermann G, van Endert PM. Concerted peptide trimming by human ERAP1 and ERAP2 aminopeptidase complexes in the endoplasmic reticulum. Nat Immunol. 2005

Seliger B, Schreiber K, Delp K, Meissner M, Hammers S, Reichert T, Pawlischko K, Tampé R, Huber C. Downregulation of the constitutive tapasin expression in human tumor cells of distinct origin and its transcriptional upregulation by cytokines. Tissue Antigens. 2001 Jan;57(1):39-45.

Seo GJ, Kim C, Shin WJ, Sklan EH, Eoh H, Jung JU. TRIM56-mediated monoubiquitination of cGAS for cytosolic DNA sensing. Nat Commun. 2018 Feb 9;9(1):613.

Seo GJ, Yang A, Tan B, Kim S, Liang Q, Choi Y, Yuan W, Feng P, Park HS, Jung JU. Akt Kinase-Mediated Checkpoint of cGAS DNA Sensing Pathway. Cell Rep. 2015 Oct 13;13(2):440-9.

Severin GB, Ramliden MS, Hawver LA, Wang K, Pell ME, Kieninger AK, Khataokar A, O'Hara BJ, Behrmann LV, Neiditch MB, Benning C, Waters CM, Ng WL. Direct activation of a phospholipase by cyclic GMP-AMP in El Tor *Vibrio cholerae*. Proc Natl Acad Sci U S A. 2018 Jun 26;115(26):E6048-E6055.

Shang G, Zhang C, Chen ZJ, Bai XC, Zhang X. Cryo-EM structures of STING reveal its mechanism of activation by cyclic GMP-AMP. Nature. 2019 Mar;567(7748):389-393.

Sharma M, Rajendrarao S, Shahani N, Ramírez-Jarquín UN, Subramaniam S. Cyclic GMP-AMP synthase promotes the inflammatory and autophagy responses in Huntington disease. Proc Natl Acad Sci U S A. 2020 Jul 7;117(27):15989-15999.

Shields MJ, Assefi N, Hodgson W, Kim EJ, Ribaudo RK. Characterization of the interactions between MHC class I subunits: a systematic approach for the engineering of higher affinity variants of beta 2-microglobulin. J Immunol. 1998 Mar 1;160(5):2297-307.

Shih AY, Damm-Ganamet KL, Mirzadegan T. Dynamic Structural Differences between Human and Mouse STING Lead to Differing Sensitivity to DMXAA. Biophys J. 2018 Jan 9;114(1):32-39.

Shoshan-Barmatz V, De S, Meir A. The Mitochondrial Voltage-Dependent Anion Channel 1, Ca^{2+} Transport, Apoptosis, and Their Regulation. Front Oncol. 2017 Apr 10;7:60.

Shu C, Yi G, Watts T, Kao CC, Li P. Structure of STING bound to cyclic di-GMP reveals the mechanism of cyclic dinucleotide recognition by the immune system. Nat Struct Mol Biol. 2012 Jun 24;19(7):722-4.

Sixt BS, Bastidas RJ, Finethy R, Baxter RM, Carpenter VK, Kroemer G, Coers J, Valdivia RH. The Chlamydia trachomatis Inclusion Membrane Protein CpoS Counteracts STING-Mediated Cellular Surveillance and Suicide Programs. Cell Host Microbe. 2017 Jan 11;21(1):113-121.

Sliter DA, Martinez J, Hao L, Chen X, Sun N, Fischer TD, Burman JL, Li Y, Zhang Z, Narendra DP, Cai H, Borsche M, Klein C, Youle RJ. Parkin and PINK1 mitigate STING-induced inflammation. Nature. 2018 Sep;561(7722):258-262.

Song S, Peng P, Tang Z, Zhao J, Wu W, Li H, Shao M, Li L, Yang C, Duan F, Zhang M, Zhang J, Wu H, Li C, Wang X, Wang H, Ruan Y, Gu J. Decreased expression of STING predicts poor prognosis in patients with gastric cancer. Sci Rep. 2017 Feb 8;7:39858.

Srikanth S, Woo JS, Wu B, El-Sherbiny YM, Leung J, Chupradit K, Rice L, Seo GJ, Calmettes G, Ramakrishna C, Cantin E, An DS, Sun R, Wu TT, Jung JU, Savic S, Gwack Y. The Ca^{2+} sensor STIM1 regulates the type I interferon response by retaining the signaling adaptor STING at the endoplasmic reticulum. Nat Immunol. 2019 Feb;20(2):152-162.

Su C, Zheng C. Herpes Simplex Virus 1 Abrogates the cGAS/STING-Mediated Cytosolic DNA-Sensing Pathway via Its Virion Host Shutoff Protein, UL41. J Virol. 2017 Feb 28;91(6):e02414-16.

Sun H, Zhang Q, Jing YY, Zhang M, Wang HY, Cai Z, Liuyu T, Zhang ZD, Xiong TC, Wu Y, Zhu QY, Yao J, Shu HB, Lin D, Zhong B. USP13 negatively regulates antiviral responses by deubiquitinating STING. Nat Commun. 2017 May 23;8:15534.

Sun L, Xing Y, Chen X, Zheng Y, Yang Y, Nichols DB, Clementz MA, Banach BS, Li K, Baker SC, Chen Z. Coronavirus papain-like proteases negatively

regulate antiviral innate immune response through disruption of STING-mediated signaling. PLoS One. 2012;7(2):e30802.

Takeuchi O, Akira S. Innate immunity to virus infection. Immunol Rev. 2009 Jan;227(1):75-86.

Takeuchi O, Akira S. Pattern recognition receptors and inflammation. Cell. 2010 Mar 19;140(6):805-20.

Takeuchi O, Akira S. Pattern recognition receptors and inflammation. Cell. 2010 Mar 19;140(6):805-20.

Tang CH, Zundell JA, Ranatunga S, Lin C, Nefedova Y, Del Valle JR, Hu CC. Agonist-Mediated Activation of STING Induces Apoptosis in Malignant B Cells. Cancer Res. 2016 Apr 15;76(8):2137-52.

Unterholzner L, Keating SE, Baran M, Horan KA, Jensen SB, Sharma S, Sirois CM, Jin T, Latz E, Xiao TS, Fitzgerald KA, Paludan SR, Bowie AG. IFI16 is an innate immune sensor for intracellular DNA. Nat Immunol. 2010 Nov;11(11):997-1004.

Van Dis E, Sogi KM, Rae CS, Sivick KE, Surh NH, Leong ML, Kanne DB, Metchette K, Leong JJ, Bruml JR, Chen V, Heydari K, Cadieux N, Evans T, McWhirter SM, Dubensky TW Jr, Portnoy DA, Stanley SA. STING-Activating Adjuvants Elicit a Th17 Immune Response and Protect against Mycobacterium tuberculosis Infection. Cell Rep. 2018 May 1;23(5):1435-1447.

Wang H, Hu S, Chen X, Shi H, Chen C, Sun L, Chen ZJ. cGAS is essential for the antitumor effect of immune checkpoint blockade. Proc Natl Acad Sci U S A. 2017 Feb 14;114(7):1637-1642.

Wang J, Yang S, Liu L, Wang H, Yang B. HTLV-1 Tax impairs K63-linked ubiquitination of STING to evade host innate immunity. Virus Res. 2017 Mar 15;232:13-21.

Wang L, Wen M, Cao X. Nuclear hnRNPA2B1 initiates and amplifies the innate immune response to DNA viruses. Science. 2019 Aug 16;365(6454):eaav0758.

Wang Q, Huang L, Hong Z, Lv Z, Mao Z, Tang Y, Kong X, Li S, Cui Y, Liu H, Zhang L, Zhang X, Jiang L, Wang C, Zhou Q. The E3 ubiquitin ligase RNF185 facilitates the cGAS-mediated innate immune response. PLoS Pathog. 2017 Mar 8;13(3):e1006264.

Wang Y, Lian Q, Yang B, Yan S, Zhou H, He L, Lin G, Lian Z, Jiang Z, Sun B. TRIM30α Is a Negative-Feedback Regulator of the Intracellular DNA and DNA Virus-Triggered Response by Targeting STING. PLoS Pathog. 2015 Jun 26;11(6):e1005012.

Wang Y, Luo J, Alu A, Han X, Wei Y, Wei X. cGAS-STING pathway in cancer biotherapy. Mol Cancer. 2020 Sep 4;19(1):136.

Warner JD, Irizarry-Caro RA, Bennion BG, Ai TL, Smith AM, Miner CA, Sakai T, Gonugunta VK, Wu J, Platt DJ, Yan N, Miner JJ. STING-associated vasculopathy develops independently of IRF3 in mice. J Exp Med. 2017 Nov 6;214(11):3279-3292.

Watson RO, Bell SL, MacDuff DA, Kimmey JM, Diner EJ, Olivas J, Vance RE, Stallings CL, Virgin HW, Cox JS. The Cytosolic Sensor cGAS Detects Mycobacterium tuberculosis DNA to Induce Type I Interferons and Activate Autophagy. Cell Host Microbe. 2015 Jun 10;17(6):811-819.

West AP, Khoury-Hanold W, Staron M, Tal MC, Pineda CM, Lang SM, Bestwick M, Duguay BA, Raimundo N, MacDuff DA, Kaech SM, Smiley JR, Means RE, Iwasaki A, Shadel GS. Mitochondrial DNA stress primes the antiviral innate immune response. Nature. 2015 Apr 23;520(7548):553-7.

West AP, Khoury-Hanold W, Staron M, Tal MC, Pineda CM, Lang SM, Bestwick M, Duguay BA, Raimundo N, MacDuff DA, Kaech SM, Smiley JR, Means RE, Iwasaki A, Shadel GS. Mitochondrial DNA stress primes the antiviral innate immune response. Nature. 2015 Apr 23;520(7548):553-7.

Whiteley AT, Eaglesham JB, de Oliveira Mann CC, Morehouse BR, Lowey B, Nieminen EA, Danilchanka O, King DS, Lee ASY, Mekalanos JJ, Kranzusch PJ. Bacterial cGAS-like enzymes synthesize diverse nucleotide signals. Nature. 2019 Mar;567(7747):194-199.

Woo SR, Fuertes MB, Corrales L, Spranger S, Furdyna MJ, Leung MY, Duggan R, Wang Y, Barber GN, Fitzgerald KA, Alegre ML, Gajewski TF. STING-dependent cytosolic DNA sensing mediates innate immune recognition of immunogenic tumors. Immunity. 2014 Nov 20;41(5):830-42.

Wu X, Wu FH, Wang X, Wang L, Siedow JN, Zhang W, Pei ZM. Molecular evolutionary and structural analysis of the cytosolic DNA sensor cGAS and STING. Nucleic Acids Res. 2014 Jul;42(13):8243-57.

Xia P, Ye B, Wang S, Zhu X, Du Y, Xiong Z, Tian Y, Fan Z. Glutamylation of the DNA sensor cGAS regulates its binding and synthase activity in antiviral immunity. Nat Immunol. 2016 Apr;17(4):369-78.

Xia T, Yi XM, Wu X, Shang J, Shu HB. PTPN1/2-mediated dephosphorylation of MITA/STING promotes its 20S proteasomal degradation and attenuates innate antiviral response. Proc Natl Acad Sci U S A. 2019 Oct 1;116(40):20063-20069.

Xie J, Li Y, Shen X, Goh G, Zhu Y, Cui J, Wang LF, Shi ZL, Zhou P. Dampened STING-Dependent Interferon Activation in Bats. Cell Host Microbe. 2018 Mar 14;23(3):297-301.e4.

Xu H, Su C, Pearson A, Mody CH, Zheng C. Herpes Simplex Virus 1 UL24 Abrogates the DNA Sensing Signal Pathway by Inhibiting NF-κB Activation. J Virol. 2017 Mar 13;91(7):e00025-17.

Ye R, Su C, Xu H, Zheng C. Herpes Simplex Virus 1 Ubiquitin-Specific Protease UL36 Abrogates NF-κB Activation in DNA Sensing Signal Pathway. J Virol. 2017 Feb 14;91(5):e02417-16.

Yi G, Wen Y, Shu C, Han Q, Konan KV, Li P, Kao CC. Hepatitis C Virus NS4B Can Suppress STING Accumulation To Evade Innate Immune Responses. J Virol. 2015 Oct 14;90(1):254-65.

Yu CH, Davidson S, Harapas CR, Hilton JB, Mlodzianoski MJ, Laohamonthonkul P, Louis C, Low RRJ, Moecking J, De Nardo D, Balka KR, Calleja DJ, Moghaddas F, Ni E, McLean CA, Samson AL, Tyebji S, Tonkin CJ, Bye CR, Turner BJ, Pepin G, Gantier MP, Rogers KL, McArthur K, Crouch PJ, Masters SL. TDP-43 Triggers Mitochondrial DNA Release via mPTP to Activate cGAS/STING in ALS. Cell. 2020 Oct 29;183(3):636-649.e18.

Zhang J, Zhao J, Xu S, Li J, He S, Zeng Y, Xie L, Xie N, Liu T, Lee K, Seo GJ, Chen L, Stabell AC, Xia Z, Sawyer SL, Jung J, Huang C, Feng P. Species-Specific Deamidation of cGAS by Herpes Simplex Virus UL37 Protein Facilitates Viral Replication. Cell Host Microbe. 2018 Aug 8;24(2):234-248.e5.

Zhang W, Zhou Q, Xu W, Cai Y, Yin Z, Gao X, Xiong S. DNA-dependent activator of interferon-regulatory factors (DAI) promotes lupus nephritis by activating the calcium pathway. J Biol Chem. 2013 May 10;288(19):13534-50.

Zhang X, Wu J, Du F, Xu H, Sun L, Chen Z, Brautigam CA, Zhang X, Chen ZJ. The cytosolic DNA sensor cGAS forms an oligomeric complex with DNA and undergoes switch-like conformational changes in the activation loop. Cell Rep. 2014 Feb 13;6(3):421-30.

Zhang Y, Chen W, Wang Y. STING is an essential regulator of heart inflammation and fibrosis in mice with pathological cardiac hypertrophy via endoplasmic reticulum (ER) stress. Biomed Pharmacother. 2020 May;125:110022.

Zhang Z, Yuan B, Bao M, Lu N, Kim T, Liu YJ. The helicase DDX41 senses intracellular DNA mediated by the adaptor STING in dendritic cells. Nat Immunol. 2011 Sep 4;12(10):959-65.

Zhong B, Zhang L, Lei C, Li Y, Mao AP, Yang Y, Wang YY, Zhang XL, Shu HB. The ubiquitin ligase RNF5 regulates antiviral responses by mediating degradation of the adaptor protein MITA. Immunity. 2009 Mar 20;30(3):397-407.

Zhou W, Whiteley AT, de Oliveira Mann CC, Morehouse BR, Nowak RP, Fischer ES, Gray NS, Mekalanos JJ, Kranzusch PJ. Structure of the Human cGAS-DNA Complex Reveals Enhanced Control of Immune Surveillance. Cell. 2018 Jul 12;174(2):300-311.e11.

The graphical abstract was created with BioRender.com.